

# 臺灣二〇〇三年國際科學展覽會

科 別：物理科

作品名稱：磁性流体薄膜在水平磁場下結構型態之研究

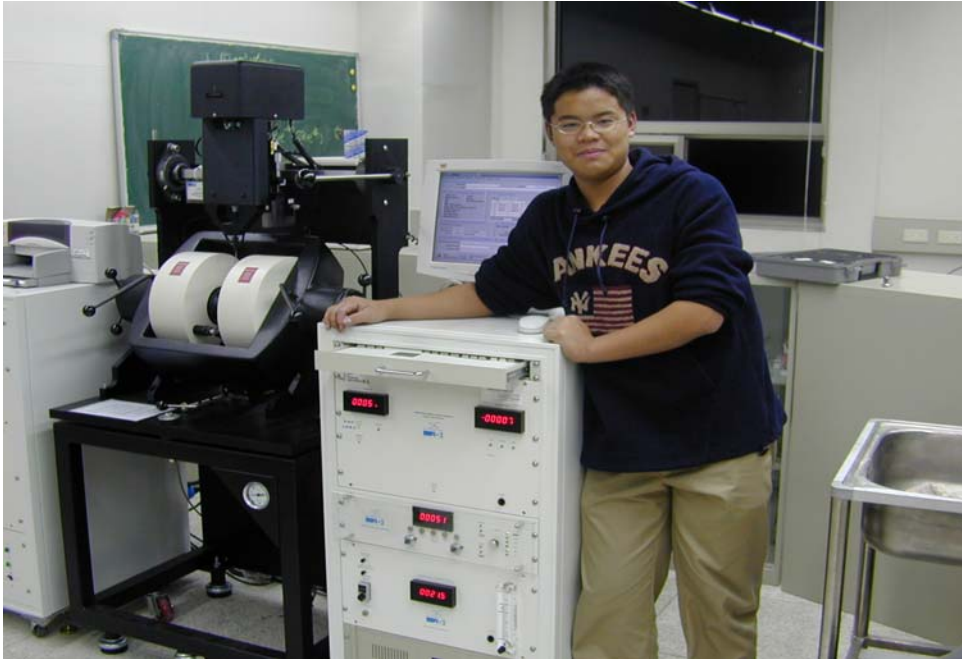
得獎獎項：物理科第二名

莫斯科二〇〇三年科學博覽會

學 校：台北市立建國高級中學

作 者：趙贊新

## 作者簡介



科學研究是一條辛苦又孤獨的路，從國中開始一路走來，個中滋味實在難以言表，很多自然現象，常常理論上講可行，指導老師也常會輕鬆的說確是如此，但實際去作，尤其要以數據證明時，就不是那麼輕鬆或簡單的事，求證過程中絞盡腦汁、挖空心思，這種辛苦無人瞭解；然而當解出難題，找出答案時，那種喜悅和興奮，也是我最大的快樂和安慰。～趙贊新～2003.2.3

## 中 文 摘 要

本研究探討不同的控制變因，對磁性流體薄膜在水平磁場下有序結構的影響。我們發現，外加水平磁場於磁流體薄膜時，會形成一維有序磁鍊排列，磁鍊間距除會隨著磁場增強而變小外，另外其條件值如磁場強度、流體濃度、磁增率、薄膜寬度及厚度等也影響磁鍊間距。其中磁增率及磁流體濃度增加會使磁鍊間距變小，而凹槽寬度及薄膜厚度增加會使磁鍊間距變大等現象。

至於其形成磁鍊的物理作用，我們假設薄膜有三種能量交互作用，即(1)磁鍊與外加磁場間的磁能 $U_{df}$ 。(2)兩條同方向磁化的磁鍊間相互排斥所造成的磁能 $U_{dd}$ 。(3)熱能 $U_{ther}$ 等。藉由系統能量 $U_{df} + U_{dd} + U_{ther}$ 最小化，我們導出了磁鍊間距和外加磁場之間理論上的關係，並比較實驗結果確實具有相當的一致性。

因這些有序結構會引發許多的光學性質，將來這些特殊的光學性質預料應可製成可調式光柵、光開關及顯示器等光電元件，使磁流體在奈米世界及光電領域裏扮演重要角色。

## Abstract

We investigate experimentally the structure of the magnetic chains formed in the magnetic fluid thin film under the influence of the external magnetic field parallel to the film surface. A one-dimensional ordered structure forced by magnetic chains can be obtained in the magnetic fluid film. It is worth noting that the ordered structure can be manipulated by changing the control parameters such as the magnetic field, concentration of magnetic fluid, the thickness of the film, the width of the film, and the  $dH/dt$ . On the other hand, the physical mechanism of forming the ordered structure can be also studied theoretically.

These magnetic chains are regarded as magnetic dipoles and three possible interactions are considered for the energy of the system: the attracting potential energy between the magnetic chain and H (denoted by  $U_{at}$ ), the repulsive potential energy between two magnetic chains with parallel magnetizations (denoted by  $U_{at}$ ), and the thermal energy  $U_{ther}$ . The relationship between the chain distance  $\Delta x$  and the applied magnetic field H was derived by minimizing the total energy of the system with respect to the chain distance. The experimental data is consistent with the theoretical results.

# 磁性流體薄膜在水平磁場下

## 結構型態之研究

### 壹、研究前言

磁性流體是一種具超順磁的流體，其中包括磁性微粒、界面活性劑及載液(如圖 1 所示)。

磁性微粒的直徑約5到10奈米，每個微粒有一與它的尺寸大小成固定比例磁矩。在未外加磁場前，這些磁性微粒藉由界面活性劑的輔助及布朗運動，均勻分散於載粒液中。

當外加磁場時，微粒磁矩會轉向順著磁場方向，微粒間因彼此相吸引而聚集排列成束。

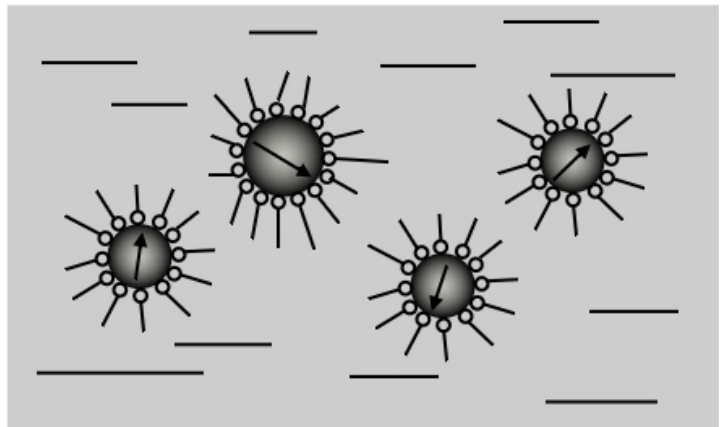


圖 1

將磁性流體封裝於矽凹槽內可成磁流體薄膜，薄膜內磁性微粒會隨著不同磁場而出現各種聚態。例如在外加垂直磁場下(磁場垂直薄膜表面)，

當磁場強度增強到某一臨界值時，磁性粒子會聚集而形成磁束，這些磁束散亂地分布在薄膜中。隨著磁場強度的增強，有愈多的磁束生成，而磁束間的作用力也隨之增強，最後這些磁束會形成一個六角形有序結構。進一



步的研究發現，此六角形有序結構可藉由調整磁場強度等控制參數來調控此有序結構。另外，此六角形有序結構會引發許多特殊的光學性質，如磁色效應及可調式穿透率。這些特殊的光學性質可被應用來製成可調式光柵，光開關及顯示器等光電元件。

另一方面在外加如水平磁場(磁場方向平行薄膜表面)下，當磁場強度大到某一臨界值時，磁性粒子會聚集成鍊狀，並會隨磁場強度的增強逐漸形成一維的有序結構排列。但現今對此有序結構的了解不多，爲了能掌握磁性流體薄膜在水平磁場下磁性鍊的排列形式，本研究將探討不同的控制變因對磁性流體薄膜在水平磁場下有序結構的影響。希望能對該週期性結構型態做更穩定地控制並進一步釐清此有序結構之相關物理作用。

## 貳、研究目的

目前對磁流體薄膜在水平磁場下有序結構特性及相關調控機制的瞭解稍嫌不足，這將嚴重影響我們對此有序結構進一步的應用研究。因此，本研究將探討磁性流體薄膜在水平磁場下的有序結構行爲。確切的研究目標擬訂如下：

- 一、瞭解磁性流體薄膜在外加水平磁場下有序結構之可調特性。
- 二、探討此可調性結構與相關控制變因間的調變關係。
- 三、釐清此可調性有序結構之物理作用機制。

## 參、研究設備及器材

### 一、研究設備

CCD、光學顯微鏡、外加場電磁鐵、電腦、矽晶片凹槽、AB膠、磁流體、蓋玻片、電源供應器、氦氖雷射、反射鏡、光檢器(detector)、玻璃光纖、電流電壓表、步進馬達、光學桌。

### 二、觀測架構

爲了達成研究目標，首先要進行的是觀測架構的建立，其中包括製作磁性流體薄膜，以及架設了結構觀測平台等。

#### (一)磁性流體薄膜的製作

要讓磁性流體薄膜在水平磁場作用下能產生有序結構，除了需有高品質的磁性流體外，另外封裝磁性流體的矽晶凹槽邊界必須陡峭、平整，若邊界不夠陡峭、平整，則磁束因邊界起起伏伏，無法成有序排列。因此我們選用矽晶圓並運用微影蝕刻技術來製作我們所需要之凹槽。製作流程如下：

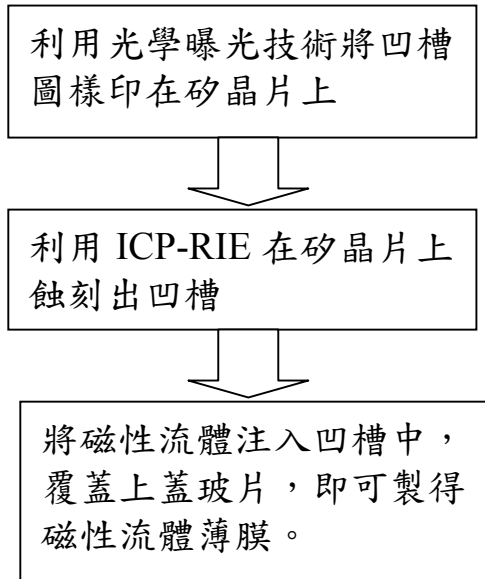
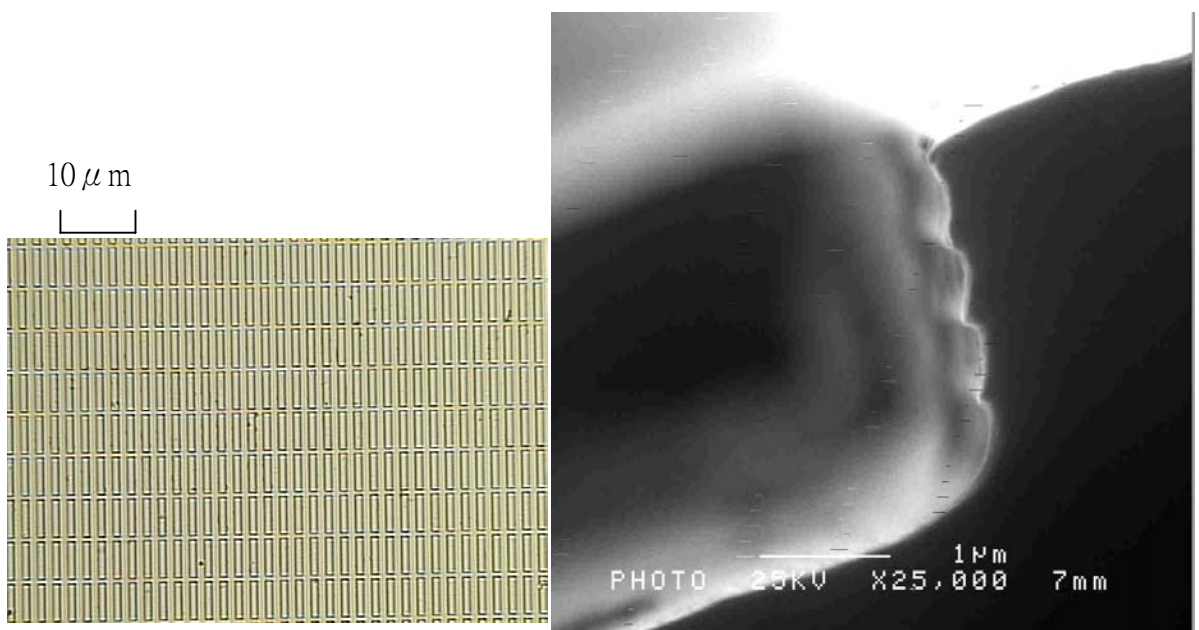


圖 2



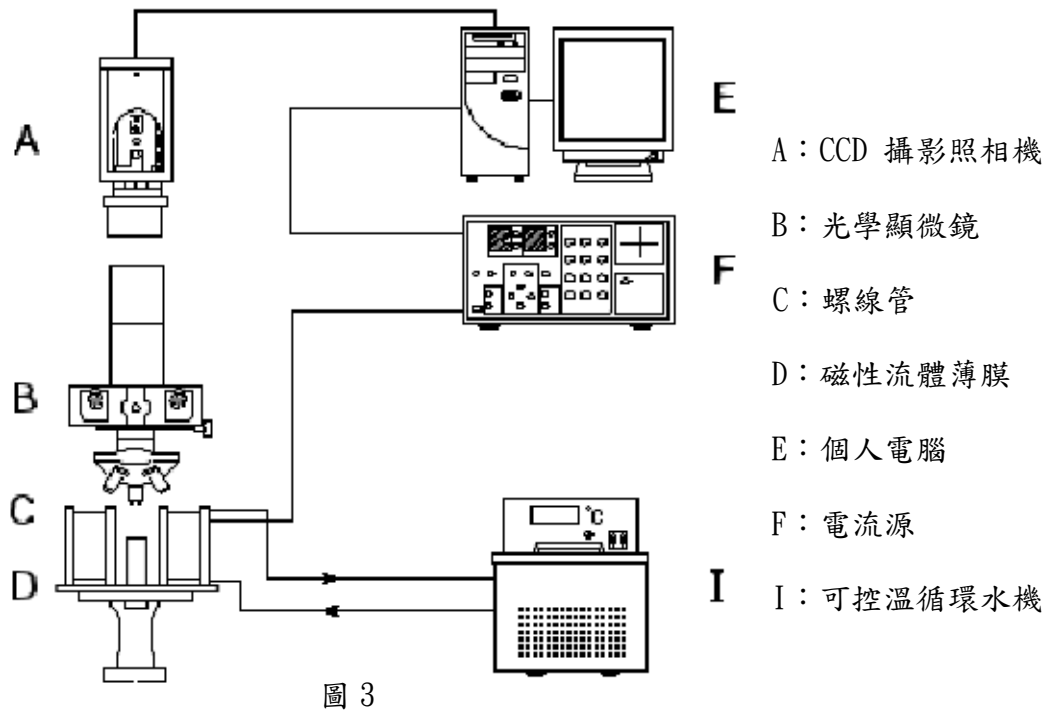
用掃描式電子顯微鏡拍攝矽晶圓所做成之凹槽放大 25000 倍圖。

註：爲了報告書寫方便，往後有關外加磁場強度、濃度、磁增率、寬度、厚度、磁鍊間距，各自以  $H$ ， $M_s$ ， $dH/dt$ ， $W$ ， $L$ ， $\Delta x$  代表度、厚度、磁鍊間距等。

(二)磁性流體薄膜結構觀測平台

磁性流體薄膜在外加水平磁場下之結構觀測平台如圖 3 所示。利用電腦程式，將參數傳輸給電源供應器，以輸出適當的電流至螺線管線圈，產生所需要的  $H$ 、 $dH/dt$  水平磁場，另外爲了避免磁鐵過熱，我們多裝一套循環水系統來控制溫度。至於影像部分經由顯微鏡，

透過 CCD 攝影照像機，將影像傳回電腦來進行拍照及攝影。



磁性流體薄膜之有序結構實驗器材設置圖

#### 肆、研究過程及方法

##### 實驗一：觀察可調性一維有序結構及H(外加磁場)對 $\Delta x$ (磁鍊距離)的影響

- 1、取磁性流體薄膜 $W=10\ \mu\text{m}$ ， $L=1.5\ \mu\text{m}$ ， $M_s=10.5\text{emu/g}$  置於兩個水平螺線圈管中。

- 2、將  $dH/dt$  固定於 5 Oe/s，改變磁場大小，觀察有序結構產生現象。
- 3、拍照及分析  $H$  (外加磁場) 對於  $\Delta x$  (磁鍊距離) 的影響。

#### 實驗二：探討 $\Delta x-H$ 特徵曲線之操縱變因

- 1、不同的  $dH/dt$  (磁增率) 對  $\Delta x-H$  的影響
  - (1) 取磁性流體薄膜  $W=10\ \mu\text{m}$ ， $L=1.5\ \mu\text{m}$ ， $M_s=10.5\text{emu/g}$  置於兩個水平螺線圈管中。
  - (2) 將  $H$  固定於 230 Oe，改變  $dH/dt$  大小，觀察有序結構產生現象。
  - (3) 拍照及分析  $dH/dt$  (磁增率) 對於  $\Delta x$  (磁鍊距離) 的影響。
- 2、不同的  $M_s$  (流體濃度) 對  $\Delta x-H$  的影響
  - (1) 取磁性流體薄膜  $W=10\ \mu\text{m}$ ， $L=1.5\ \mu\text{m}$ ，置於兩個水平螺線圈管中。
  - (2) 將  $H$  固定於 230 Oe， $dH/dt$  固定於 5 Oe/s，改變  $M_s$  濃度大小，觀察有序結構產生現象。
  - (3) 拍照及分析  $M_s$  對於  $\Delta x$  (磁鍊距離) 的影響。
- 3、不同的  $W$  (凹槽寬度) 對  $\Delta x-H$  的影響
  - (1) 取磁性流體薄膜  $L=1.5\ \mu\text{m}$ ， $M_s=10.5\text{emu/g}$ ，置於兩個水平螺線圈管中。
  - (2) 將  $H$  固定於 230 Oe， $dH/dt$  固定於 5 Oe/s，改變  $W$  (寬度) 大小，觀察有序結構產生現象。
  - (3) 拍照及分析  $W$  對於  $\Delta x$  (磁鍊距離) 的影響。
- 4、不同的  $L$  (薄膜厚度) 對  $\Delta x-H$  的影響
  - (1) 取磁性流體薄膜  $W=10\ \mu\text{m}$ ， $M_s=10.5\text{emu/g}$ ，置於兩個水平螺線圈管中。
  - (2) 將  $H$  固定於 230 Oe， $dH/dt$  固定於 5 Oe/s，改變  $L$  (厚度) 大小，觀察有序結構產生現象。
  - (3) 拍照及分析  $L$  對於  $\Delta x$  (磁鍊距離) 的影響。

## 伍、結果

#### 實驗一、可調性一維有序結構及 $\Delta x-H$ 特徵曲線：

當磁場以固定的磁增率  $dH/dt$ ，由零增大到某一強度時，我們發現原本分散於液體中的磁性粒子會開始聚集成磁鍊。起初這些磁鍊是散亂的分布在薄膜內，當磁場繼續增強時，磁鍊數目愈來愈多，磁鍊間的作用力愈來愈強。而當磁場強度到達某臨界值時，這些磁鍊形成一維有序排列，圖 4(a)  $\Delta x$  代表此有序結構的週期。隨著磁場的增強，有更多的磁鍊產生，因此磁鍊間距會越少。圖 4 中  $\Delta x$  與磁場的變化關係繪於圖 5。值得注意的是，所觀察到的一組有序結構是單層的。

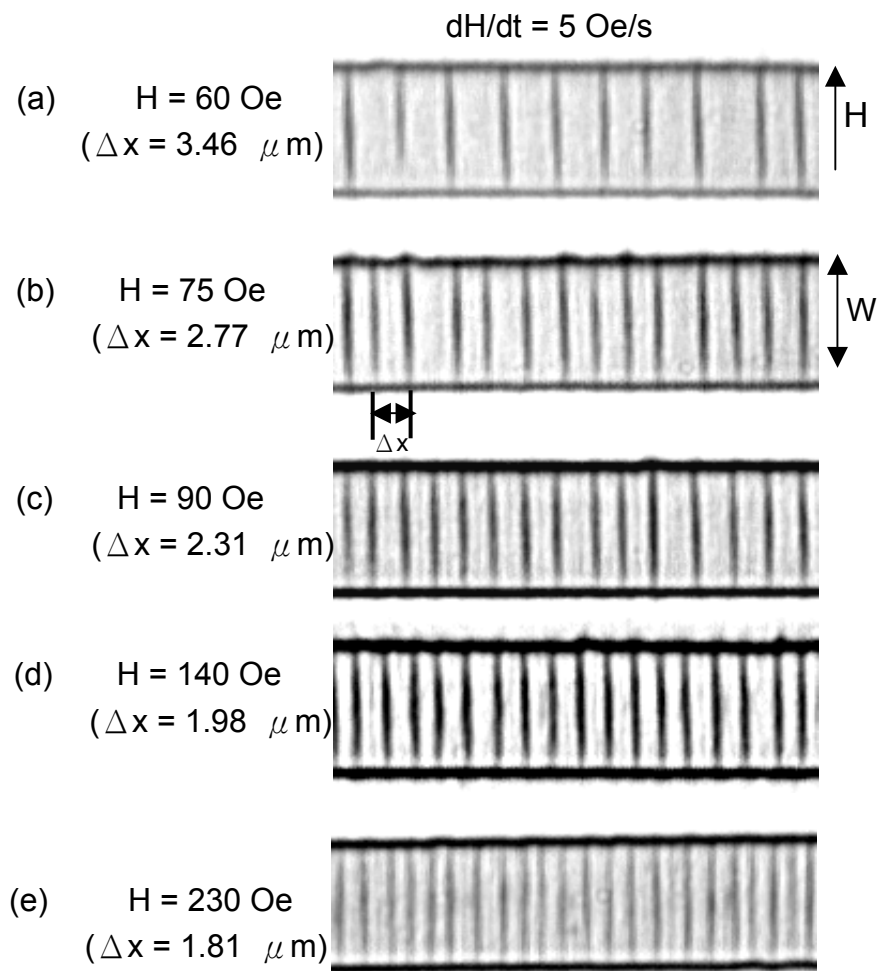


圖 4

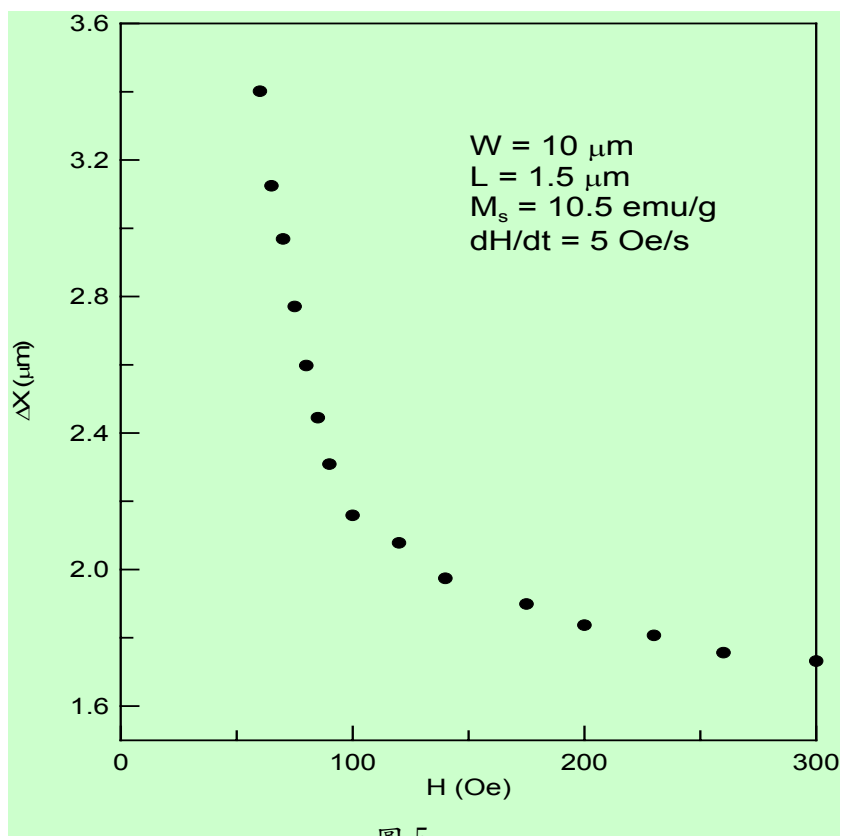


圖 5

## 實驗二、 $\Delta x-H$ 特徵曲線之操縱變因探討：

在以下實驗(實驗二)中我們試著找出控制  $\Delta x-H$  特徵曲線的方法。

### (一)不同 $dH/dt$ (磁增率)對 $\Delta x-H$ 特徵曲線的影響：

當使用不同的大小的磁增率  $dH/dt$  增強磁場並同時觀察磁性薄膜內的一維有序結構改變，我們可以明顯的看出其週期性結構排列的變化： $dH/dt$  越大時， $\Delta x-H$  曲線會往左下方移動，如圖 6 所示。這表示對一個固定磁場強度而言， $dH/dt$  越大， $\Delta x$  會降低。此結果之原因可由圖 7 看出當  $dH/dt$  愈大時，所形成的磁鍊較細，磁矩也較小，磁鍊的排斥較小，因此其有序結構的週期  $\Delta x$  也會隨之降低。

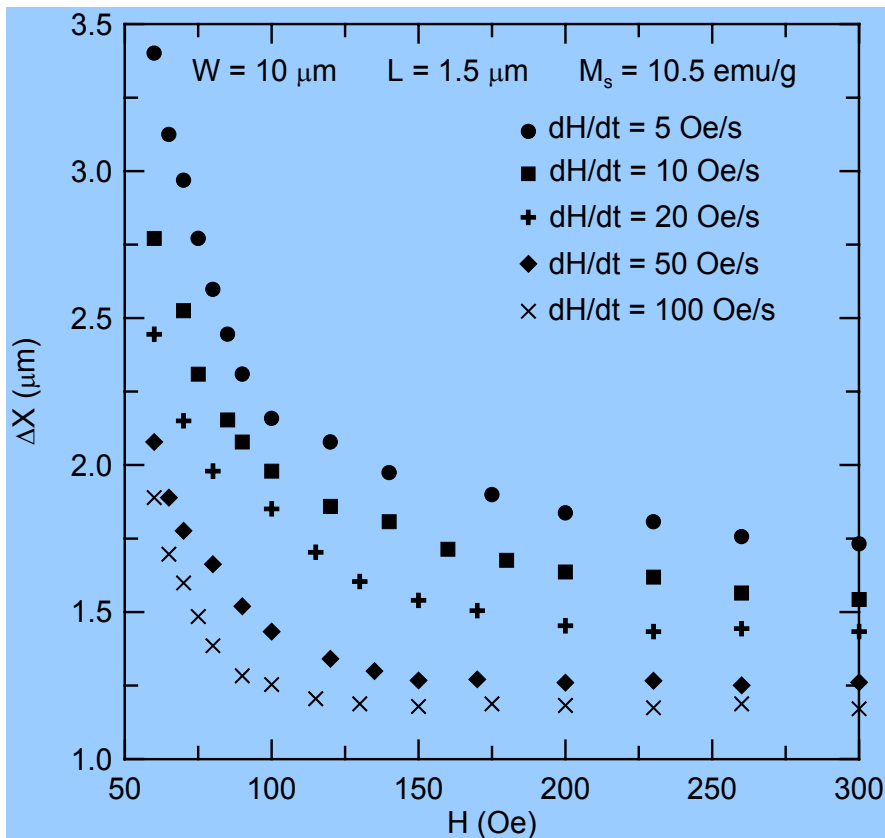
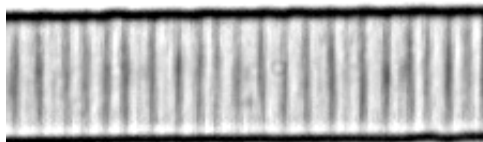


圖 6

(a)  $H = 230$  Oe  
 $dH/dt = 5$  Oe/s



(b)  $H = 230$  Oe  
 $dH/dt = 10$  Oe/s



(c)  $H = 230$  Oe  
 $dH/dt = 100$  Oe/s

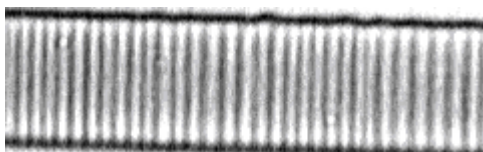


圖 7

(二) 不同  $M_s$ (流體濃度)對  $\Delta x-H$  特徵曲線的影響：

當濃度  $M_s$  越大時， $\Delta x-H$  曲線會往左下方移動，如圖 8 所示。這表示對一個固定磁場強度而言，濃度  $M_s$  越大， $\Delta x$  會降低。此結果之原因可由圖 9 看出磁性流體濃度愈高，所形成的磁鍊較細，磁矩也較小，磁鍊的排斥較小，因此其有序結構的週期  $\Delta x$  也會隨之降低。

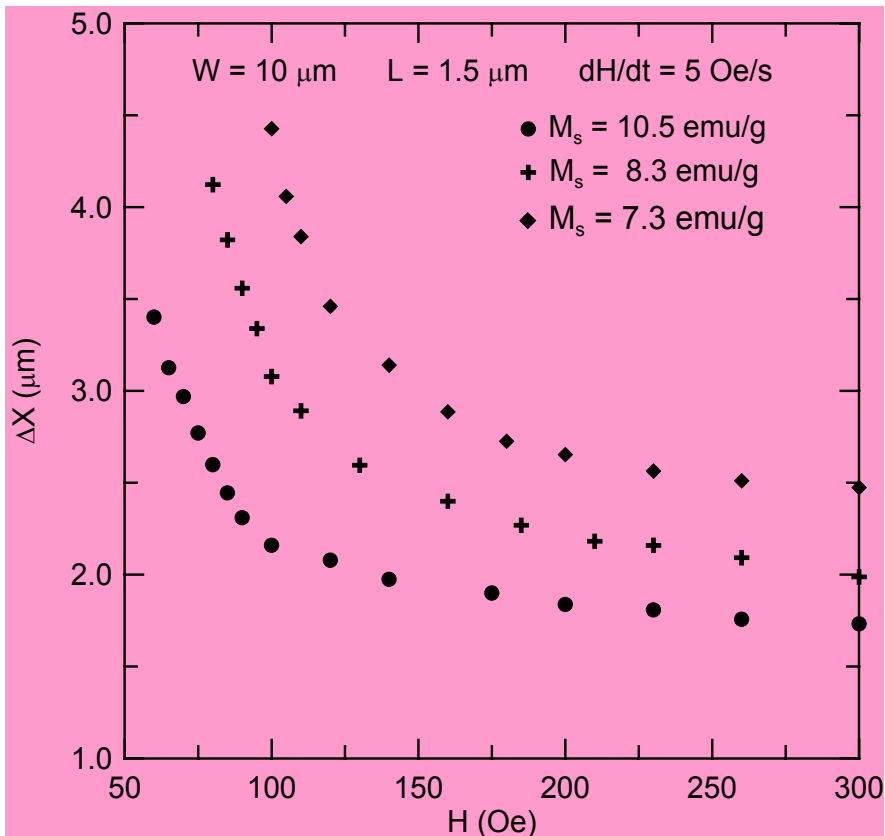


圖 8

(a)  $H = 230$  Oe

$M_s = 7.3$  emu/g

(b)  $H = 230$  Oe

$M_s = 8.3$  emu/g

(c)  $H = 230$  Oe

$M_s = 10.5$  emu/g

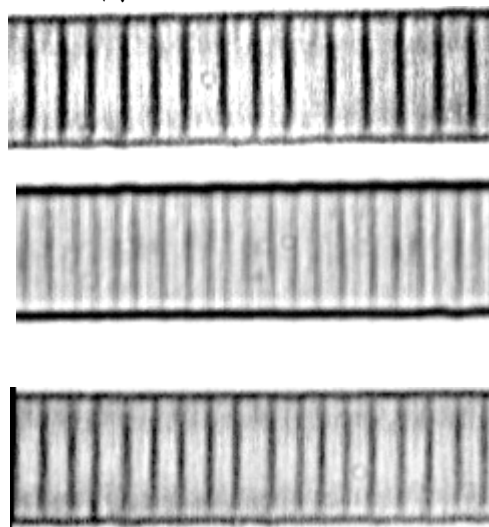


圖 9

(三) 不同  $W$ (凹槽寬度)對  $\Delta x-H$  特徵曲線的影響：

觀察不同凹槽寬度  $W$  之磁性流體薄膜在水平磁場下的有序結構。這裡所使用的凹槽寬度有  $5$ 、 $10$  及  $20 \mu\text{m}$ ，我們發現當凹槽寬度  $W$  越大時， $\Delta x-H$  曲線會往右上方移動，如圖 10 所示。這表示對一個固定磁場強度而言，凹槽寬度  $W$  越大時， $\Delta x$  會昇高。此結果之原因可由圖 11 看出凹槽寬度較寬時，磁鍊較粗，磁矩也較大，磁鍊的排斥較大，因此其有序結構的週期  $\Delta x$  也會隨之升高。

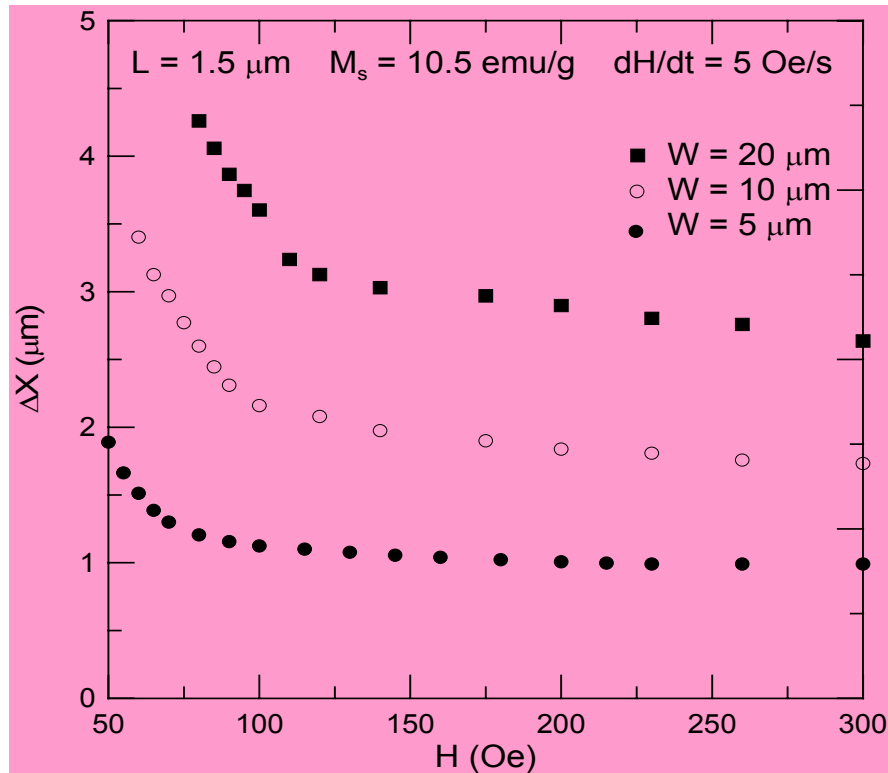


圖 10

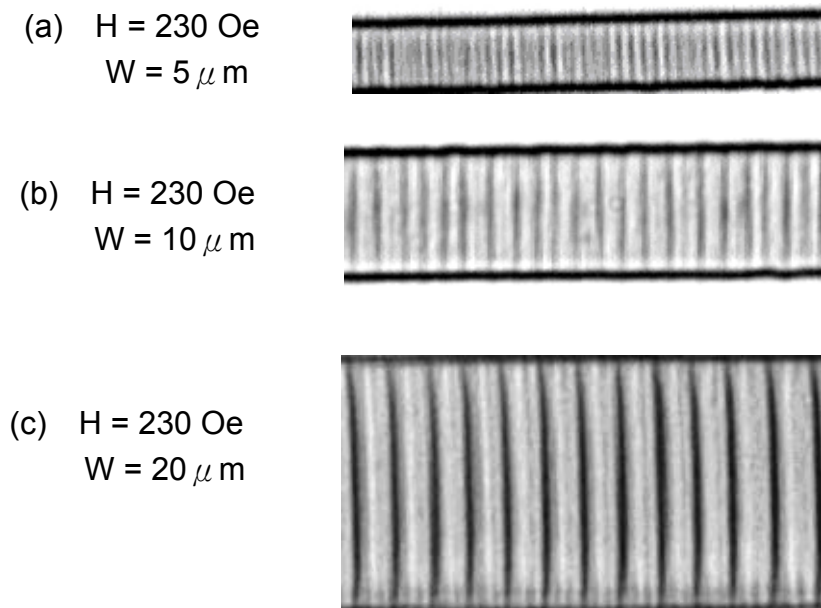


圖 11

(四) 不同 L(薄膜厚度)對  $\Delta x-H$  特徵曲線的影響：

爲了保證磁性流體薄膜在水平磁場下之有序結構是單層，我們除了觀察凹槽厚度爲  $1.5 \mu\text{m}$  之薄膜中的結構外，另使用更薄的凹槽厚度( $0.5 \mu\text{m}$ )來進行。我們發現當 L(薄膜厚度)越大時， $\Delta x-H$  曲線會往右上方移動，如圖 12 所示。這表示對一個固定磁場強度而言，L(薄膜厚度)越大時， $\Delta x$  會升高。此結果之原因可由圖 13 看出磁鍊較細，磁矩也較小，磁鍊的排斥較小，因此其有序結構的週期  $\Delta x$  也會隨之降低。

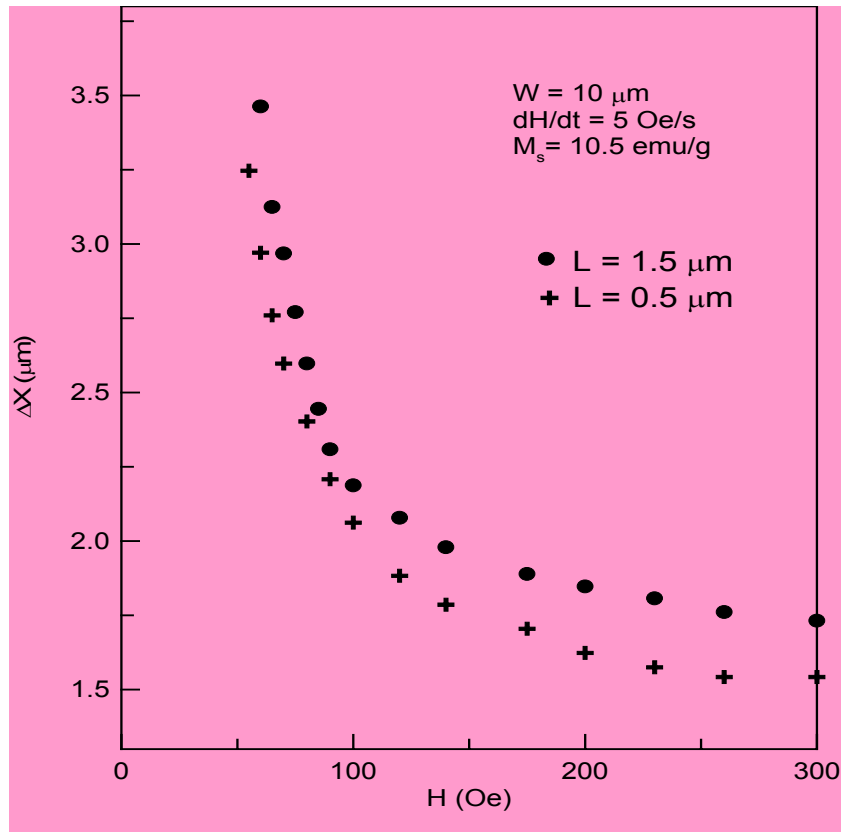


圖 12

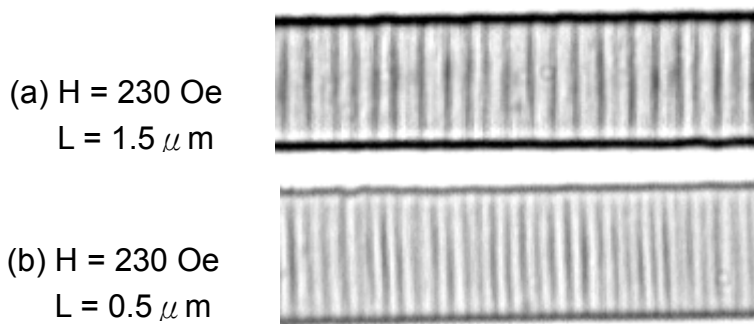


圖 13

## 陸、結果討論--結構排列理論探討

### 一、理論模式

磁性流體薄膜在外加水平磁場下之一維有序結構中，有三種可能的交互作用產生：(一)磁鍊與外加磁場間的磁能  $U_{dH}$ ，(二)由於兩條同方向磁化的磁鍊間相互排斥所造成的磁能  $U_{dd}$  以及(三)熱能  $U_{ther}$  等。因此該系統總能量為  $U_{dH} + U_{dd} + U_{ther}$ ，而磁鍊間距和外加磁場之間的關係，藉由將總能量最小化來導出，以下我們將分別算出各項能量。

首先，我們討論熱能對於總能量的貢獻。一個自由微粒在室溫下的熱能估計會有  $10^{-14}$ erg，( $U_{ther}=3k_B T/2$ ， $k_B$  是 Boltzmann 常數， $T$  是溫度)而對一個磁化率是  $302.4\text{emu/cm}^3$  直徑為  $100\text{\AA}$  的  $\text{Fe}_3\text{O}_4$  磁性微粒，每個微粒的磁力矩為  $m_p=1.6\times 10^{-16}\text{emu}$ [7,8]。如此，一個磁微粒與外加磁場 ( $80\sim 250\text{Oe}$ )之間的磁位能約為  $10^{-14}$ erg，與熱能約為一樣的大小，這表示熱能在總能量中是不可忽視的。但要注意的是，磁微粒是懸在液體裏，流體會大大降低磁性微粒的熱運動，因而會使熱能的影響變得很小。因此，可在總能量中將熱能的影響略去。在以下對總能量  $U_T$  理論計算中只考慮磁位能  $U_{dH}$  和  $U_{dd}$ 。

假設薄膜的面積是無限的，裏面的有序結構是一致的，每單位面積的總磁位能  $U_T$  可表如下：

$$U_T = U_{dH} + U_{dd} = n u_{dH} + \frac{1}{2} \sum_{j=1}^n \sum_{\substack{i=1 \\ i \neq j}}^N u_{dd} (|R_i - R_j|) \dots\dots\dots(1)$$

$n$  是每單位長度磁鍊個數。

$N$  是薄膜內磁鍊之總數。

$u_{dH}$  表示在外加磁場  $H$  之下每個磁鍊之磁位能。

$U_{dd}(R_i - R_j)$  是位於  $R_i$  與  $R_j$  兩磁鍊之間的磁位能( $R_i$  代表第  $i$  鍊的向量位置)。既然磁流體的磁鍊磁化方向平行於外加磁場  $H$ ，每個磁鍊的  $U_{dH}$  能量應如下：

$$u_{dH} = -\kappa M H = -\kappa M H \dots\dots\dots(2)$$

$\kappa (\leq 1)$  表示反磁化效應。

$M$  表示每一磁鍊的磁力矩(magnetic moment)。

從方程式(2)，我們定義出每個磁鍊之有效磁力矩  $M_{eff} = \kappa M$ ，其中隱含著每一磁鍊的磁力矩包含了反磁化效應。因此， $U_{dH}$  可寫成  $U_{dH} = -M_{eff} H$ ，而每個磁鍊磁力矩可表如下：

$$M_{eff} = b m_p \dots\dots\dots(3)$$

b 為常數代表每磁鍊內磁性微粒個數， $m_p$  是每個磁微粒的有效磁力矩，對於一個固定的  $dH/dt$ ，我們觀察到磁鍊大小不會隨磁場大小而改變，這表示在固定  $dH/dt$  下，不管磁場強度大小，每個磁鍊中的磁微粒個數是不變的。另一方面，兩平行磁化之磁鍊間的排斥磁位能，方程式 (1) 中的  $U_{dd}$  所示：

$$U_{dd} = \frac{1}{2} \sum_{j=1}^n \sum_{\substack{i=1 \\ i \neq j}}^N u_{dd} (|R_i - R_j|) \dots\dots\dots (4)$$

上式中，對於  $i$  的加總代表選定第  $j$  個磁鍊與其他磁鍊間的磁位能總和。由於有序結構是週期性的， $R_i - R_j$  將會是某些值，因此，所選定的  $j$  磁鍊與其它磁鍊間的磁能如下：

$$\sum_{\substack{i=1 \\ i \neq j}}^N u_{dd} (|R_i - R_j|) = \sum_k \xi_k u_{dd}^k (\rho_k) \dots\dots\dots (5)$$

$u_{dd}^k (\rho_k)$  為任何兩個相距  $\rho_k$  長磁鍊的磁位能，因此， $U_{dd}$  在方程式(4)中變為：

$$U_{dd} = \frac{1}{2} \sum_{j=1}^n \sum_k \xi_k u_{dd}^k (\rho_k) = \frac{n}{2} \sum_k \xi_k u_{dd}^k (\rho_k) \dots\dots\dots (6)$$

從方程式(2)及(6)中，總磁位能的密度  $U_T$  從(1)中變為

$$U_T = U_{dH} + U_{dd} = -nM_{eff}H + \frac{n}{2} \sum_k \xi_k u_{dd}^k (\rho_k) \dots\dots\dots (7)$$

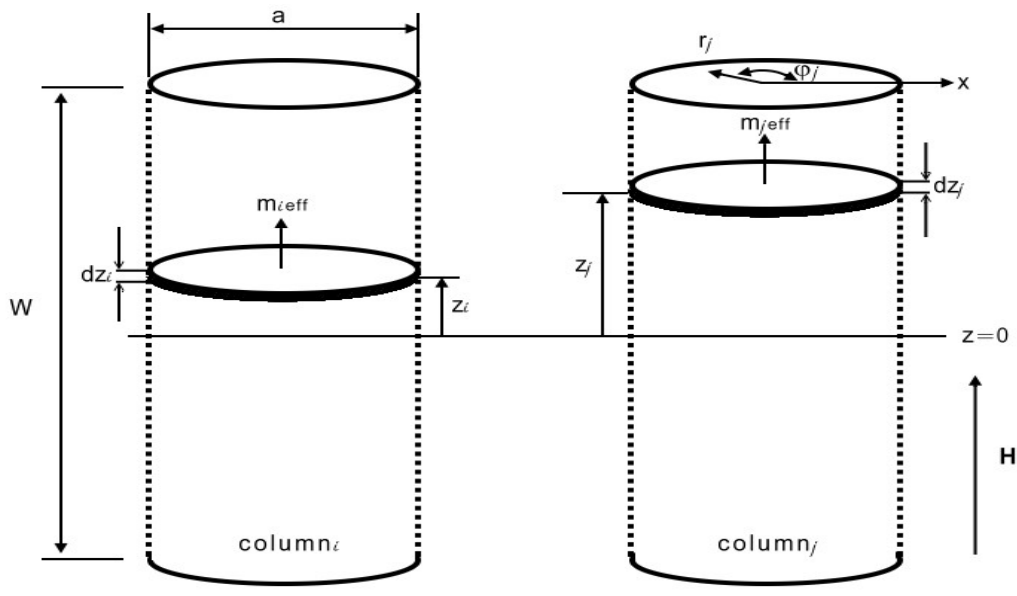
在兩個最相近的第  $k$ -th(參考磁鍊  $i$  和  $j$ )相距  $\rho_k$  長的磁鍊間的磁位能  $u_{dd}^k (\rho_k)$  如方程式(6)，根據參考資料〔6〕的定義可計算出如下：

$$u_{dd}^k (\rho_k) = - \int_j H_{ij} (\rho_k) \bullet dM_{j\text{eff}} \dots\dots\dots (8)$$

$H_{ij}$  代表磁鍊  $i$  從磁鍊  $j$  的某一定點所產生的磁場強度。

$dM_{j\text{eff}}$  表示磁鍊  $j$  中的某一段的有效磁力矩。

而其總合的區間加總仍在磁鍊  $j$  內，在方程式(8)中， $u_{dd}^k$  係根據於每個磁鍊內磁性微粒的分配尚仍不明，在本研究的理論計算中，我們假設定在磁鍊內的磁力矩是均勻分佈的。



磁偶極示意圖

圖 1 4

我們先假設磁鍊為圓柱形，如圖 14 所示，再將磁鍊分成不同的薄層，並算出此兩薄層間的磁位能，其次在  $z_i$  和  $z_j$  兩個層之間的磁位能  $du_{dd}^k(\rho_k)$  ( $M_{ieff}$  和  $M_{jef}$  相對的磁力矩) 亦可算出。

循著  $z$  軸方向在兩個磁鍊之內的高度，將其積分可得  $du_{dd}^k(\rho_k)$ ，因此， $u_{dd}^k(\rho_k)$  可計算如下：

$$u_{dd}^k(\rho_k) = \int_{z_i = -\frac{w}{2}}^{\frac{w}{2}} \int_{z_j = -\frac{w}{2}}^{\frac{w}{2}} du_{dd}^k \dots\dots\dots(9)$$

$$du_{dd}^k = - \int_{m_j} h_{ij} \cdot dm_{jef}$$

$w$  是磁鍊的長度。

$h_{ij}$  是由  $m_{jef}$  產生在  $M_{ieff}$  位置上的磁場

$dM_{jef}$  乃是  $m_{jef}$  中一個小薄層的磁力矩，既然每個磁鍊的磁化乃是延著  $z$  軸，磁場  $h_{ij}$  僅考慮

軸方向的組成。並寫出如下：

$$h_{i,z} = \frac{\pi I a^2}{c} \left\{ \frac{-1}{\left( (z_j - z_i)^2 + \rho_k^2 + r_j^2 + 2\rho_k r_j \cos\phi_j \right)^{3/2}} + \dots \right.$$

$$\left. \frac{3(z_j - z_i)^2}{\left( (z_j - z_i)^2 + \rho_k^2 + r_j^2 + 2\rho_k r_j \cos\varphi_j \right)^{5/2}} \right\} \dots\dots\dots(10)$$

$I = (cM_{\text{eff}} \pi a^2 w) dz_i$  和  $\left( (z_i - z_j)^2 + \rho_k^2 + r_j^2 + 2\rho_k r_j \cos\varphi_j \right)^{1/2} > a$ ， $w$  是薄膜的厚度， $r_j$  和  $\rho_k$  是  $M_{\text{eff}}$  層的

的極軸，因此， $du_{dd}^k(\rho_k)$  成爲：

$$du_{dd}^k(\rho_k) = \frac{2M_{\text{eff}}^2}{\pi a^2 w} dz_i dz_j \int_{r_j=0}^a \int_{\varphi_j=0}^{\pi} \left\{ \frac{1}{\left( (z_j - z_i)^2 + \rho_k^2 + r_j^2 + 2\rho_k r_j \cos\varphi_j \right)^{3/2}} - \frac{3(z_j - z_i)^2}{\left( (z_j - z_i)^2 + \rho_k^2 + r_j^2 + 2\rho_k r_j \cos\varphi_j \right)^{5/2}} \right\} r_j dr_j d\varphi_j \dots\dots\dots(11)$$

將方程式(9)和(11)代入方程式(7)中，每單位面積的總磁位能  $U_T$  如下：

$$U_T = \frac{-2\sqrt{3}M_{\text{eff}}H}{3\rho_1^2} + \frac{2\sqrt{3}M_{\text{eff}}^2}{3\pi\rho_1^2 a^2 w^2} \sum_k \xi_k \int_{z_i=-w/2}^{w/2} \int_{z_j=-w/2}^{w/2} \int_{r_j=0}^a \int_{\varphi_j=0}^{\pi} \left\{ \frac{1}{\left( (z_j - z_i)^2 + \rho_k^2 + r_j^2 + 2\rho_k r_j \cos\varphi_j \right)^{3/2}} - \frac{3(z_j - z_i)^2}{\left( (z_j - z_i)^2 + \rho_k^2 + r_j^2 + 2\rho_k r_j \cos\varphi_j \right)^{5/2}} \right\} r_j dr_j d\varphi_j dz_j dz_i \dots\dots\dots(12)$$

$q_k = (r_j^2 + 2\rho_k r_j \cos\varphi_j) / \left( (z_j - z_i)^2 + \rho_k^2 \right)$ ，由於磁鍊的週期性  $\rho_k$  可表成  $\rho_1$ ，因此， $U_T$  成爲  $\rho_1$  和

$H$  的方程式，所以磁鍊間的距離和  $H$  的關係可藉由  $U_T$

相對於  $\rho_1$  的極小化而得到

$$H = M_{\text{eff}}(a, W, d) \dots\dots\dots(13)$$

$M_{\text{eff}}$  代表每個磁鍊的磁力矩。

$W$  代表薄膜寬度。  $d$  代表兩磁鍊間距及實驗中  $\Delta \times$

$F$  是  $a, w, d$  的函數。

## 二、結果與討論

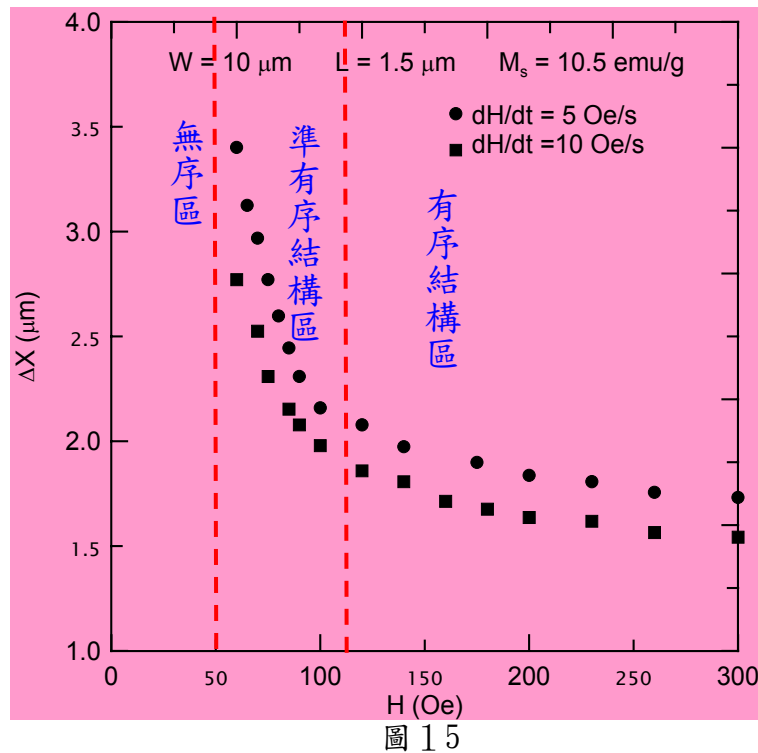


圖 15

如圖 15，經由比較研究，我們由實驗中發現，當  $H$  介於 50-120 Oe 時，結構排列並不是完整的有序結構，直到  $H$  大於 120 Oe 時，其排列才會趨於完整的有序排列，所以在理論計算中都以  $H$  大於 120 Oe 時的資料為主。每個磁鍊的磁力矩在兩個最近的磁鍊之間實驗上的磁鍊距，可藉由理論上的計算得出。

我們將實驗所獲得的數據，代入公式(13)，並求出其正比回歸算出  $M_{\text{eff}}$ ，如圖 16 虛線部分。由實驗數據與由公式(13)所獲得的虛線間相符合的結果可確定本系統中的物理作用主要是(1)磁鍊與外加磁場間的磁能  $U_{\text{dH}}$ 。(2)兩條同方向磁化的磁鍊間相互排斥所造成的磁能  $U_{\text{dd}}$ 。另外，由於  $M_{\text{eff}}$  是磁鍊的磁力矩，所以  $M_{\text{eff}}$  越大，磁鍊就越粗。 $dH/dt = 5 \text{ Oe/s} > dH/dt = 10 \text{ Oe/s}$  的  $M_{\text{eff}}$ 。 $dH/dt = 5 \text{ Oe/s}$  的磁鍊比較粗，與實驗符合。

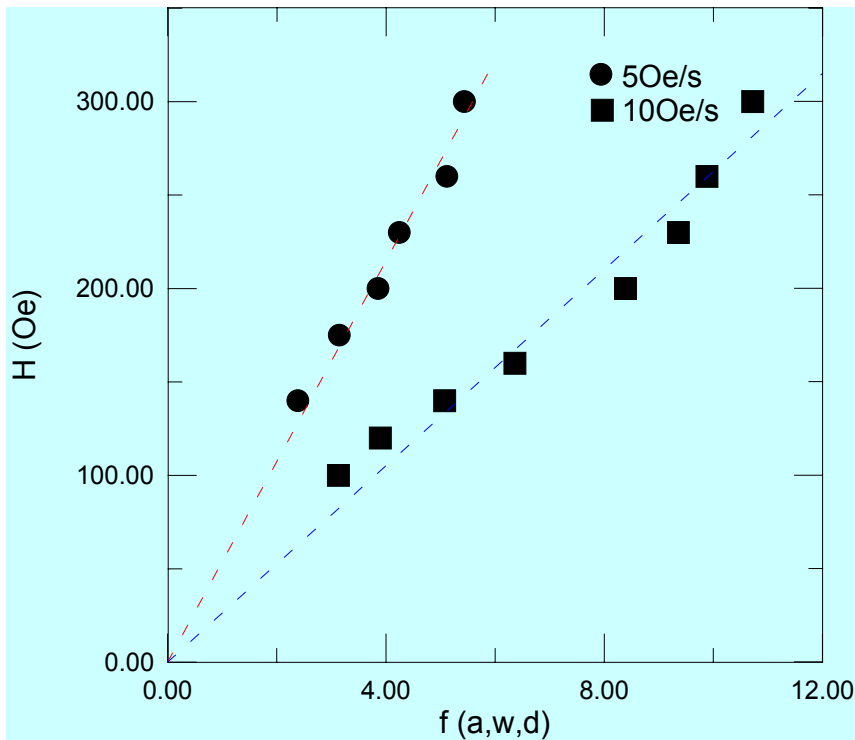


圖 16

在方程式(13)中，所得參數  $M_{\text{eff}}$  的值後，我們可畫出  $\Delta x(H)$  理論曲線如圖 17 虛線。因此，實驗所得資料比對理論曲線我們獲得了相當具有一致性的結果。

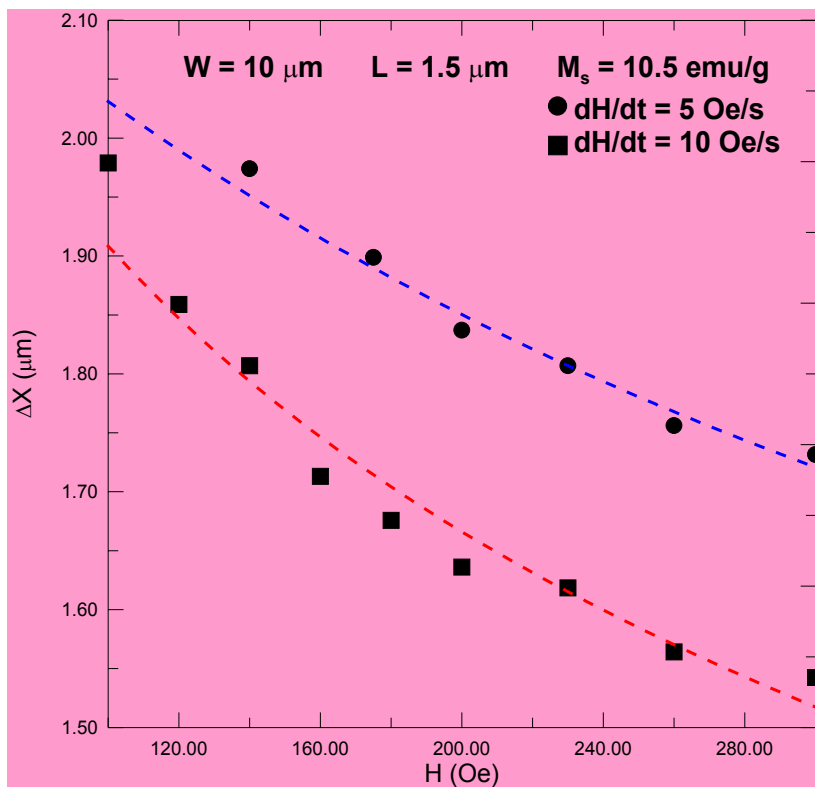


圖 17

## 柒、結論：

- 一、在磁性流體薄膜觀察到可調性一維有序結構。
- 二、該有序結構可藉由增加  $H$ (外加磁場)、 $dH/dt$ (磁增率)、 $M_s$ (流體濃度)或 減少  $W$ (凹槽寬度)及  $L$ (薄膜厚度)等操縱變因來降低結構週期  $\Delta x$ 。
- 三、藉由理論上的計算和實驗結果比較，我們確定系統中擁有兩大物理作用(1)磁鍊與外加磁場間的磁能  $U_{\text{dH}}$ 。(2)兩條同方向磁化的磁鍊間相互排斥所造成的磁能  $U_{\text{dd}}$ 。

## 捌、展望與應用

目前世界各國對於磁性流體雖然投入了相當的關注和研究，相關理論和特性也陸續被發覺和彙集，然而截至目前人類對於磁流體的應用仍相當侷限，睽其因應是人類對於磁流體的重要、關鍵特性仍未揭開，惟從我們一系列的研究中，發現它在薄膜內會產生有序結構，而這些有序結構會引發許多的光學性質，如磁效應及可調式穿透率等，這些特殊的光學性質預料應可被製成可調式光柵、光開關及顯示器等光電元件，因此，世人對於磁流體只要稍加關注，稍予研究投入，預料它將可在奈米世界及光電領域裏扮演重要角色。國人除拭目以待外，更應不落人後積極參與研究，盼望為我國科技產業開創另一片天。

## 玖：參考資料

- 1.黃忠良 磁性流體理論應用 台北市 復華出版社 民 88
- 2.Herng-Er Horng, S.Y. Yang, S.L. Lee, Chin-Yih Hong, and H.C. Yang, “Magnetochromatics of the magnetic fluid film under a dynamic magnetic field” , Appl. Phys. Letter., **79**, 350(2001)(7 月).
- 3.Chin-Yih Hong, Chun-Hui Chen, H.E. Horng, S.Y. Yang, C. A. Chen, and H.C. Yang, “Effect of initial states on the phase diagram of the structural pattern in magnetic fluid films under perpendicular magnetic field” , Appl. Phys. Letter., **79**, 2360(2001)(10 月).
- 4.H.E. Horng, C.Y. Hong, S.L. Lee, C.H. Ho, S.Y. Yang and H.C. Yang, “Magnetochromatics Resulted from Optical Gratings of Magnetic Fluid Films Subjected to Perpendicular Magnetic Fields” , J. Appl. Phys., **88**, 5904(2000)(11 月)
- 5.Chin-Yih Hong, I.J.Jang, H.E.Horng, C.J. Hsu, Y.D.Yao and H.C.Yang, “Ordered Structures in  $\text{Fe}_3\text{O}_4$  Kerosene-based Ferrofluids” , J. Appl. Phys., **81**, 275(1997). (4 月)

6. Jackson J.D. Classical Electrodynamics.-2nd ed. Ch.5.-John Wiley & Sons,1978.

7. Heng-Er Horng, Chin-Yih Hong, Wai Bong Yeung, and Hong-Chang Yang, “Magneto chromatic effects in magnetic fluid thin films” , Applied Optics, **37**, 2674(1998). (5 月)

8. Chin-Yih Hong, H.E. Horng, I.J.Jang, J.M. Wu, S.L. Lee, Wai Bong Yeung, and H.C. Yang, “Magneto-Chromatic Effects of Tunable Magnetic Fluid Grating” , J. Appl. Phys., **83**, 6771(1998). (6 月).

## Abstract

We investigate experimentally the structure of the magnetic chains formed in the magnetic fluid thin film under the influence of the external magnetic field parallel to the film surface. A one-dimensional ordered structure forced by magnetic chains can be obtained in the magnetic fluid film. It is worth noting that the ordered structure can be manipulated by changing the control parameters such as the magnetic field, concentration of magnetic fluid, the thickness of the film, the width of the film, and the  $dH/dt$ . On the other hand, the physical mechanism of forming the ordered structure can be also studied theoretically.

These magnetic chains are regarded as magnetic dipoles and three possible interactions are considered for the energy of the system: the attracting potential energy between the magnetic chain and H (denoted by  $U_{cH}$ ), the repulsive potential energy between two magnetic chains with parallel magnetizations (denoted by  $U_{cc}$ ), and the thermal energy  $U_{\text{ther}}$ . The relationship between the chain distance  $\Delta x$  and the applied magnetic field H was derived by minimizing the total energy of the system with respect to the chain distance. The experimental data is consistent with the theoretical results.

# **Tunable Ordered Structures of Magnetic Fluid Films under parallel magnetic fields**

## **I. Introduction**

Due to the rich variety of phenomena under external magnetic fields, magnetic fluid films have attracted a great deal of interest of scientists and engineers. Of these, several researchers have reported agglomeration of magnetic particles in the magnetic fluid film when a uniform magnetic field is applied.<sup>1-3</sup> Another study discussed the thermodynamics of the particle agglomeration.<sup>4</sup> In 1997, a hexagonal ordered structure in a highly homogeneous magnetic fluid film under uniform magnetic fields perpendicular to the film was found by Horng and Hong.<sup>5</sup> Subsequently, a structural evolution that followed a sequence of monodispersion, disordered state, 1<sup>st</sup>-level ordered structure, transition state and then to a 2<sup>nd</sup>-level ordered state in the magnetic fluid film was observed when the externally perpendicular field was increased.<sup>6,7</sup> It was further indicated that this structural evolution can be effectively manipulated by controlling the parameters, such as the sweep rate of the field, the film thickness, the fluid concentration, and the temperature.<sup>8,9</sup> These magnetically induced structural patterns generated several significant magneto-optics of magnetic fluid films, for example magneto-chromatics,<sup>10,11</sup> field-modulated transmission<sup>12</sup> and tunable refractive index.<sup>13</sup> These magneto-optical effects showed promising opportunities to develop magnetic-fluid-based optical gratings,<sup>14</sup> optical modulators,<sup>15</sup> optical switches,<sup>16</sup> etc.

In contrast to the ordered structure in the magnetic fluid film under perpendicular fields, the magnetic chains are distributed randomly in the magnetic fluid films under uniform parallel fields.<sup>17-19</sup> These magnetic chains induce an optical anisotropy, and hence a birefringence phenomenon can be observed in a magnetic fluid film under parallel magnetic fields when a linearly polarized light is incident into the film.<sup>17-19</sup> It was also demonstrated that the birefringence of magnetic fluid films can be further utilized as optical switches.<sup>15</sup>

According to the structures observed in the magnetic fluid film under parallel fields, there is a high degree of inhomogeneity in the length of chains formed in a wide cell. Hence, the interaction among magnetic chains is neither isotropic nor homogeneous, which contributes to the random distribution of the chains in films under parallel fields. In this work, by reducing the dimensions of the cell containing magnetic fluid using lithography technology, a formation of an ordered structure in the magnetic fluid film under parallel fields is demonstrated. In addition to investigating the structures in the magnetic fluid micro-cell, the tunability of the ordered structure and its physical intuition are also discussed.

## **II. Research Purposes**

At present, the knowledge on the features and the relevant adjusting and controlling mechanism of the ordered structure of the magnetic fluid film under parallel magnetic field are deficient in a degree, which will influence seriously the further applied research for this ordered structure. Hence, this study will investigate the ordered structure behaviors of the

magnetic fluid film under the parallel magnetic field. The definite research purposes are determined as follows:

- A、To find out the tunable features of the ordered structure in the magnetic fluid film under parallel magnetic fields.
- B、To investigate the covariant relationship between the tunable structure and the controlling factors.
- C、To clarified the physical intuition of the tunable structure.

### **III. Devices used in the study**

The magnetic fluid used here was kerosene-based  $\text{MnFe}_2\text{O}_4$  magnetic fluid with a concentration of 10.5 emu/g and was prepared by the chemical co-precipitation method. To form a magnetic fluid micro-strip, the ferrofluid was injected into a thin-strip cell and then covered with a glass plate, as illustrated in Fig. 1. In this work, the cell was made of a silicon wafer. Through a standard photo-lithographic process with the aid of ICP-RIE, a rectangular micro-strip cell of 1.5- $\mu\text{m}$  in depth and 10- $\mu\text{m}$  in width was obtained on the silicon wafer. The magnetic fluid thin film was then put into a pair of solenoids, which generated magnetic fields parallel to the plane of the film. An optical microscope and a CCD camera were used to record the structures in the magnetic fluid micro-strip. The details of manufacturing magnetic fluid micro-strips and observation platform for the structural patterns are described separately as follows.

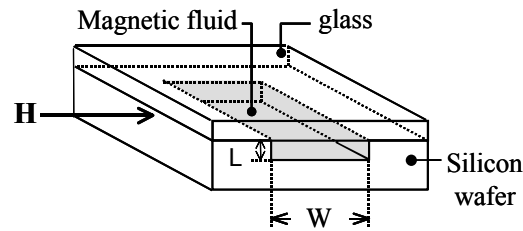
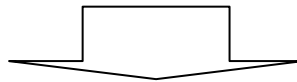


Fig.1. Scheme of the cell for the magnetic fluid micro-strip. L denotes the depth of the cell, W is the width of the cell.

### (I) Manufacture the magnetic fluid film

For the magnetic fluid film under the parallel magnetic field to produce the ordered structure, it requires the magnetic fluid of high quality as well as a steep and straight boundary for the cell encapsulating the magnetic fluid, as the flux would fail to form an ordered arrangement if the border is not smooth enough. Therefore, we use the silicon wafers to manufacture the required cell by the photolithography technique, and the manufacturing flow is as follows:

**Print the cell pattern in the silicon wafers using the optical exposure technique**



**Etch out the cell in the silicon wafers using ICP-RIE(fig.2.)**



**Inject the magnetic fluid into the cell and lay the cover glass on it, and the magnetic fluid shall be produced.**

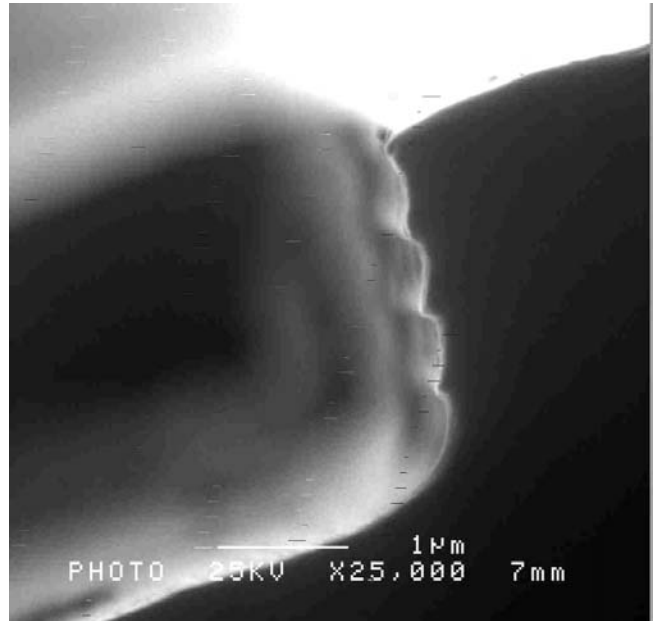
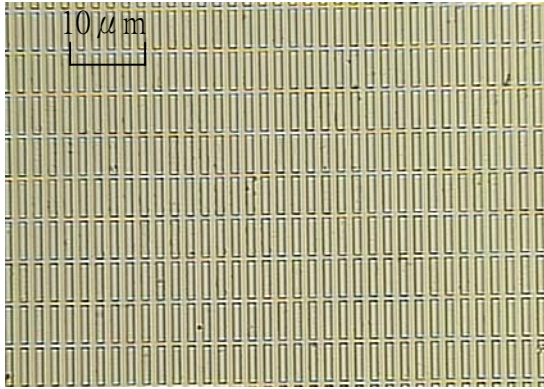


Fig.2. Photograph the silicon wafer fillister using the scanning electron microscope  $\times 25,000$

Note: For ease of writing this report, we define the symbols as follows:

$H$ —External field strength;  $M_s$ —Concentration of the magnetic fluid;

$dH/dt$ —Magnetic field sweeping rate;  $W$ —Cell width;  $L$ —Film

thickness;  $\Delta x$ —Chain spacing °

## (II) Structure observing platform for magnetic fluid film

Under the external parallel magnetic field, the structure-observing platform for magnetic fluid film is shown in Fig. 3. Using the computer program, the parameters were transmitted to the power supply to output the correct power to the solenoid coils and to obtain the parallel magnetic field with required  $H$  and  $dH/dt$ . Moreover, to avoid overheating the magnet, we install an additional water circulating system to control the temperature. The images would be photographed by transferring back to the computer with the CCD camera through the microscope.

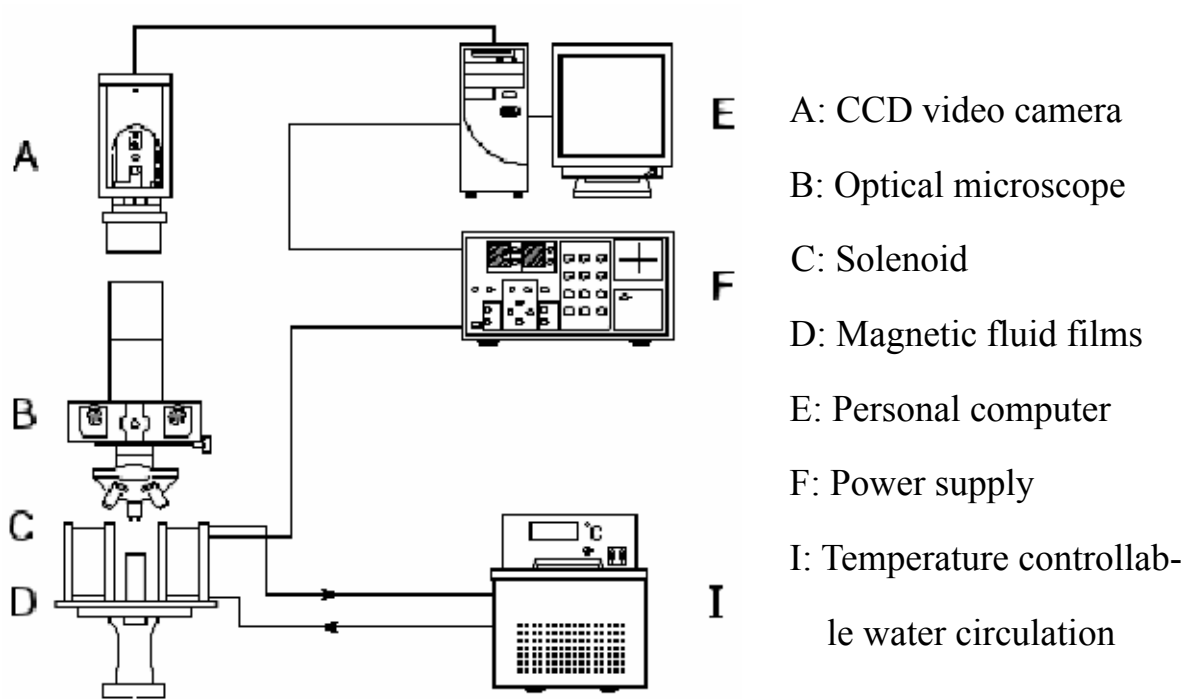


Fig.3. The device arrangement in the experiment for the ordered structure of the magnetic fluid film

## IV. Procedures and methods

Experiment 1: To observe the tunable one-dimensional ordered structure in magnetic fluid films.

1. Prepare magnetic fluid films:  $W=10\mu\text{m}$ ,  $L=1.5\mu\text{m}$ ,  $M_s=10.5\text{emu/g}$ . Lay them in two parallel solenoids.
2. Fix  $dH/dt$  at 5 Oe/s, and then change the field strength, to observe formation of the ordered structure.
3. Photograph and analyze the influence of  $H$  (external magnetic field) on  $\Delta x$  (chain spacing).

Experiment 2: To investigate the influencing factors of  $\Delta x$  - $H$  characteristic curve

### (A) The influence of different $dH/dt$ on $\Delta x$ - $H$ curve

1. Prepare magnetic fluid films:  $W=10\mu\text{m}$ ,  $L=1.5\mu\text{m}$ ,  $M_s=10.5\text{emu/g}$ . Lay them in two parallel solenoids.
2. Fix  $H$  at 230 Oe, and then change  $dH/dt$ , to observe formation of the ordered structure.
3. Photograph and analyze the influence of  $dH/dt$ (magnetic field sweeping rate) on  $\Delta x$  (chain spacing).

### (B) The influence of different $M_s$ on $\Delta x$ - $H$ curve

1. Prepare magnetic fluid films:  $W=10\mu\text{m}$ ,  $L=1.5\mu\text{m}$ . Lay them in two parallel solenoids.
2. Fix  $H$  at 230 Oe,  $dH/dt$  at 5 Oe/s, and then change  $M_s$  to observe

formation of the ordered structure.

3. Photograph and analyze the influence of  $M_s$  (concentration of the magnetic fluid) on  $\Delta x$  (chain spacing).

### (C) The influence of different $W$ on $\Delta x - H$ curve

1. Prepare magnetic fluid films:  $L = 1.5\mu\text{m}$ ,  $M_s = 10.5\text{emu/g}$ . Lay them in two parallel solenoids.
2. Fix  $H$  at 230 Oe,  $dH/dt$  at 5 Oe/s, then change  $W$  to observe formation of the ordered structure.
3. Photograph and analyze the influence of  $W$  (cell width) on  $\Delta x$  (chain spacing).

### (D) The influence of different $L$ on $\Delta x - H$ curve

1. Prepare magnetic fluid films:  $W = 10\mu\text{m}$ ,  $M_s = 10.5\text{emu/g}$ . Lay them in two parallel solenoids.
2. Fix  $H$  at 230 Oe,  $dH/dt$  at 5 Oe/s, and then change  $L$  to observe formation of the ordered structure.
3. Photograph and analyze the influence of  $L$  (film thickness) on  $\Delta x$  (chain spacing).

## V. Experimental Results

### Experiment 1: To observe the tunable one-dimensional ordered structure in magnetic fluid films.

When the magnetic field increased from zero to certain intensity in a fixed  $dH/dt$ , we found that the magnetic particles formerly dispersing in the fluid would aggregate into magnetic

chains. In the beginning, these magnetic chains distributed within the film randomly, and when the magnetic field increased continuously, the number of magnetic chains increased also, and the operating force between magnetic chains was stronger and stronger. While the magnetic density arrived at a certain threshold, these magnetic chains were arranged in one dimension, as shown in Fig. 4(a), where  $\Delta x$  represents the average period of this ordered structure. With the strength of the magnetic field increasing, more magnetic chains were emerged, thus the chain spacing was reduced. The dependent relationship between  $\Delta x$  and the magnetic field in Fig.4 was shown in Fig.5. It is necessary to note that the observed ordered structure was a single layer structure.

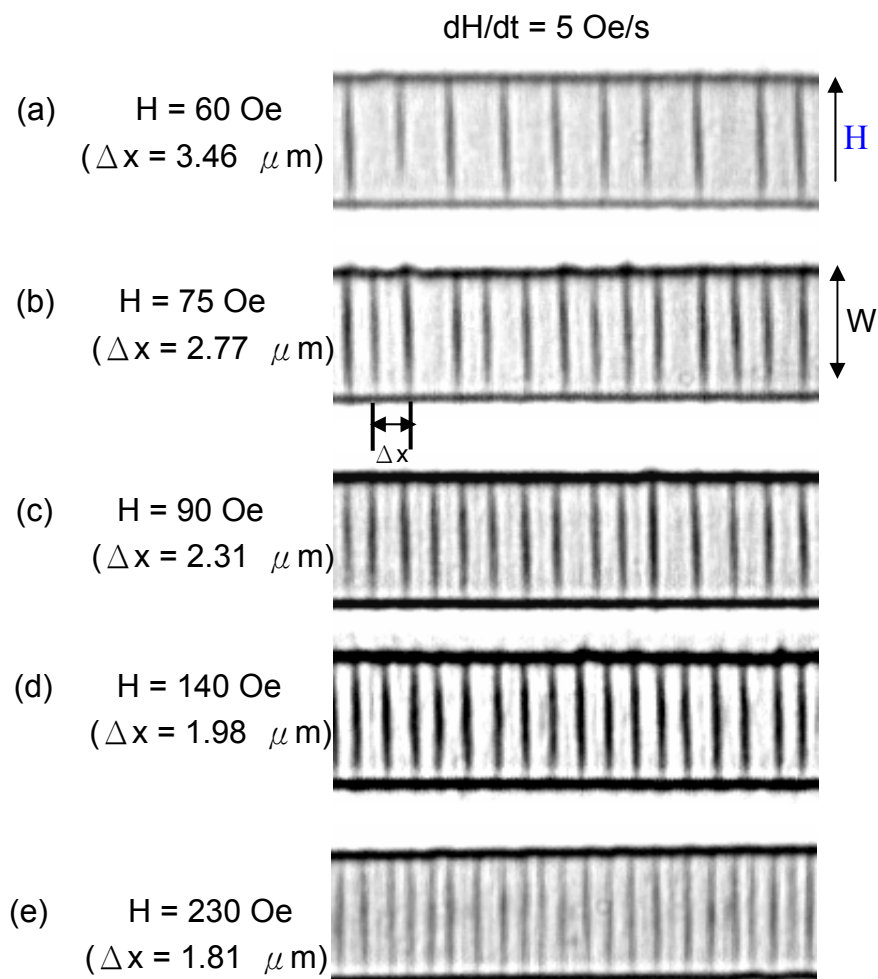


Fig.4. Periodic chain structures under various parallel fields

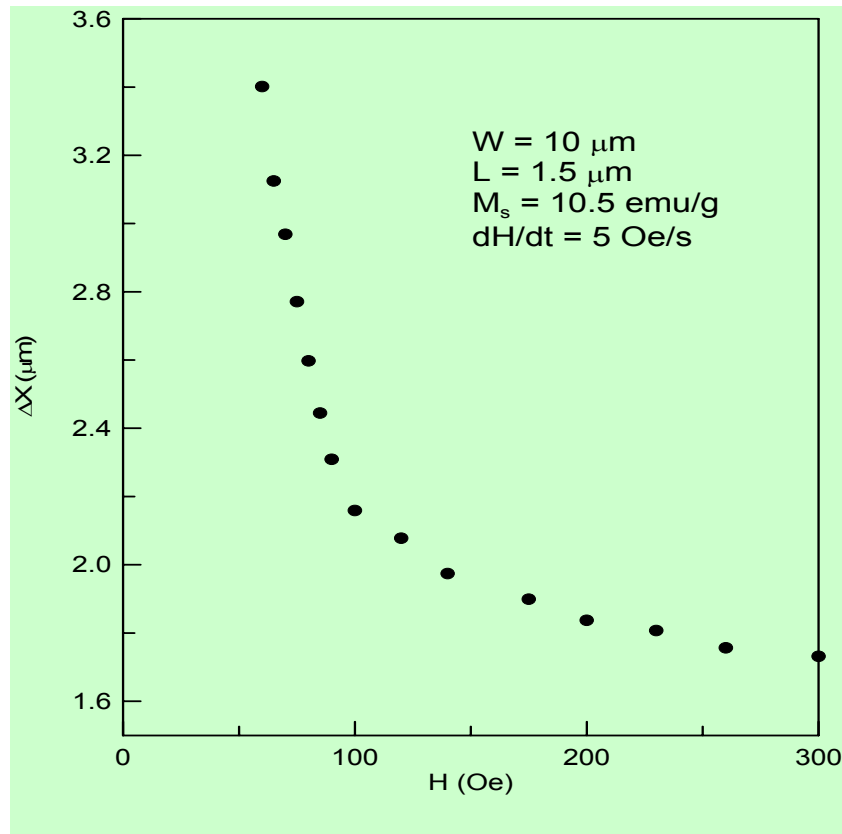


Fig.5. When the magnetic field increasing, the chain spacing was reduced

In the following experiment (experiment 2),we try to find out the method to control the  $\Delta x - H$  characteristic curve.

### Experiment 2: To investigate the influencing factors of $\Delta x - H$ characteristic curve

#### (A) The influence on characteristic $\Delta x - H$ curve at different $dH/dt$ 's

First of all, the effect of the sweep rate,  $dH/dt$ , on the  $\Delta x - H$  curve is investigated. When  $dH/dt$  is increased, the  $\Delta x - H$  curve moves toward the lower left, as shown in Fig.6, The results mean that, under a fixed field strength, the higher the sweeping rate( $dH/dt$ ), the smaller the chain spacing. The cause

for this result could be interpreted by comparing the structural patterns under a given  $H$  for various  $dH/dt$ 's, as shown in Fig.7. When  $dH/dt$  is higher, the magnetic chain is thinner, Thus, the magnetic moment is smaller, and in turns the repulsion between the magnetic chains is lower. Consequently, the  $\Delta x$  of this ordered structure would decrease at a higher  $dH/dt$ .

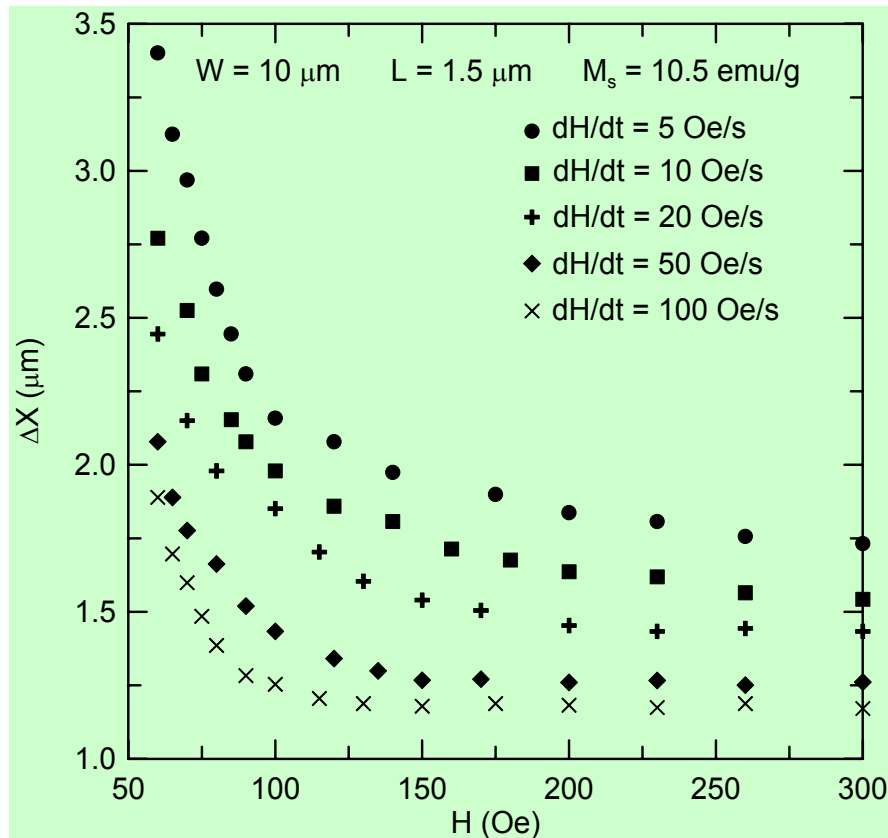


Fig.6.  $\Delta x$ - $H$  curve moves toward the lower left, when  $dH/dt$  is increased

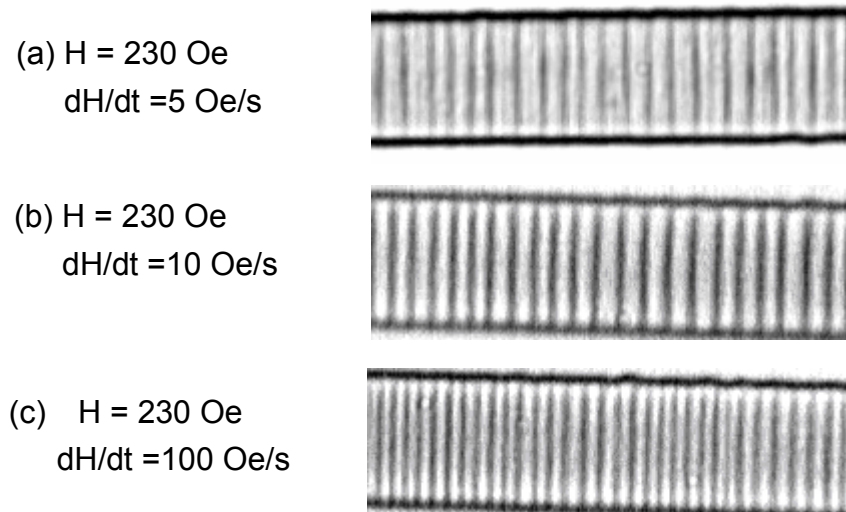


Fig.7. Periodic chain under a given  $H$  for various  $dH/dt$

## (B) The influence of $M_s$ on $\Delta x$ -H curve

When  $M_s$  is increased, the  $\Delta x$  -H curve moves toward the lower left, as shown in Fig.8, having a fixed field strength, the higher the concentration( $M_s$ ), the smaller the chain spacing becomes. The cause for this result could be seen in Fig.9. When  $M_s$  is higher, the magnetic chain is thinner, the magnetic moment is smaller, and the repulsion between the magnetic chains is lower, so the period  $\Delta x$ , of this ordered structure would decrease as a result.

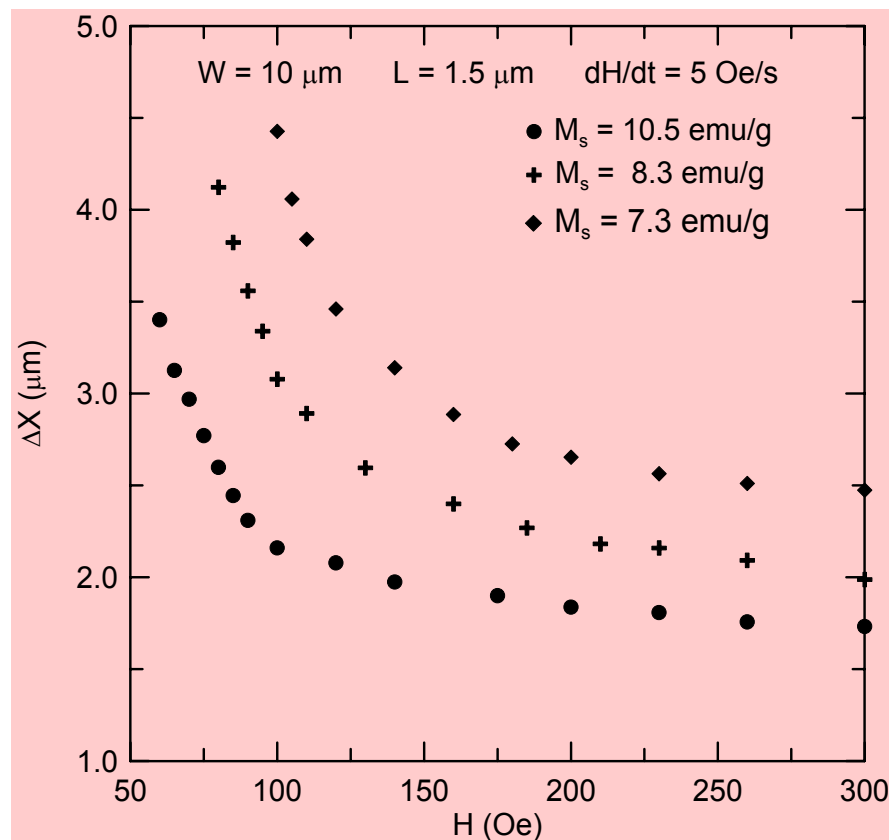


Fig.8.  $\Delta x$ -H curve moves toward the lower left, when  $M_s$  is increased

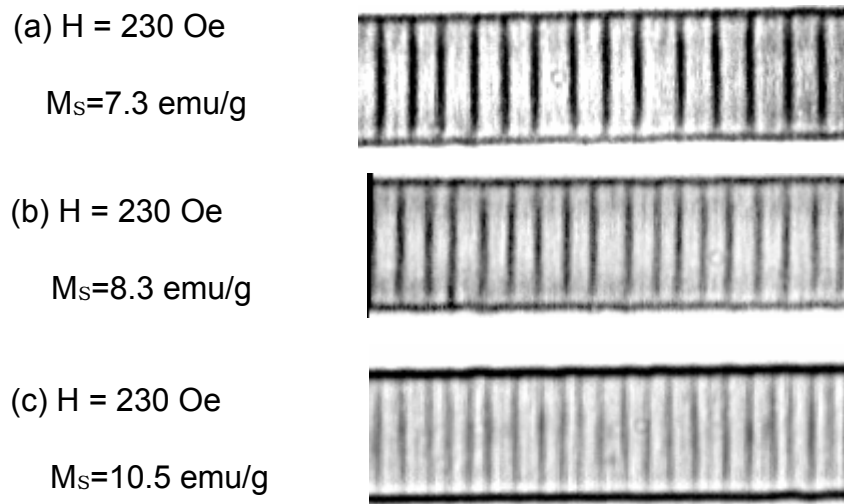


Fig.9. Periodic chain under a given  $H$  for various  $M_s$

### (C) The influence of $W$ on $\Delta x - H$ curve

When using different  $W$  (5, 10 and  $20\mu\text{m}$ ) and observing the ordered structure in the magnetic film under the parallel magnetic field. We could find that when  $W$  is increased, the  $\Delta x - H$  curve moves toward the upper right, as shown in Fig.10, having a fixed field strength, a bigger cell width( $w$ ), the higher the chain spacing becomes. The cause for this result could be seen in Fig.11. When  $W$  is bigger, the magnetic chain is thicker, the magnetic moment is bigger, and the repulsion between the magnetic chains is higher, so the circle  $\Delta x$  of this ordered structure would increase as a result.

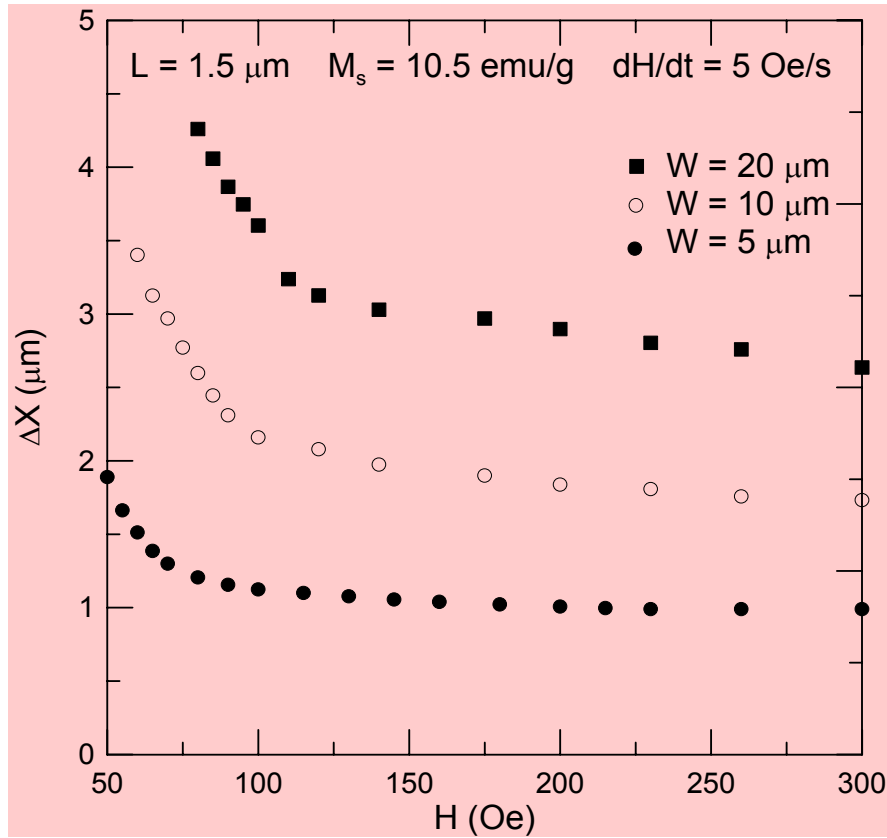


Fig.10.  $\Delta x$ -H curve moves toward the upper right, when W is increased

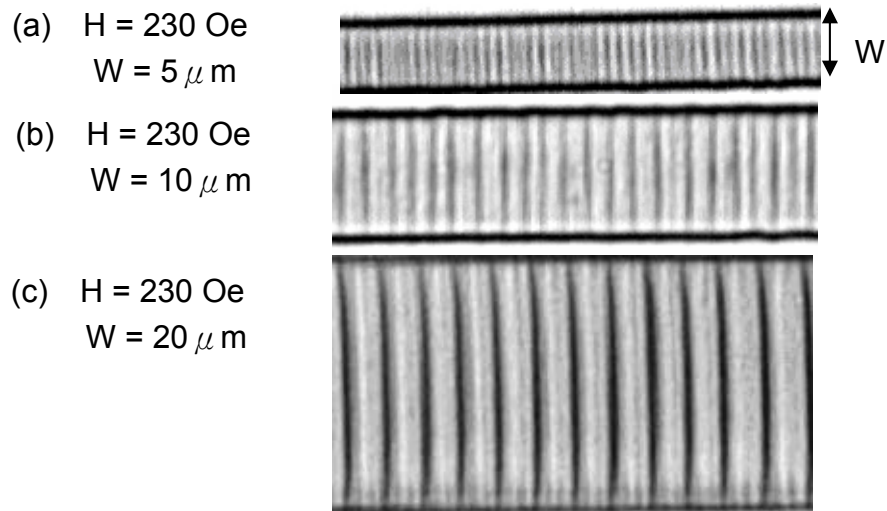


Fig.11. Periodic chain under a given H for various W

### (D) The influence of L on $\Delta x$ -H curve

To ensure a single layer ordered structure in the magnetic film under the parallel magnetic field, we performed the study using thinner cell ( $L=0.5\mu\text{m}$ ) as well as using the thickness of

1.5 $\mu\text{m}$ . We found that when  $L$  is decreased, the  $\Delta x$  - $H$  curve moves toward the lower left, as shown in Fig.12, having a fixed field strength, a smaller film thickness, the lower chain spacing( $\Delta x$ )becomes. The cause for this result could be seen in Fig.13. When  $L$  is smaller, the magnetic chain is thinner, the magnetic moment is smaller, and the repulsion between the magnetic chains is lower, so the circle  $\Delta x$  of this ordered structure is decrease as a result.

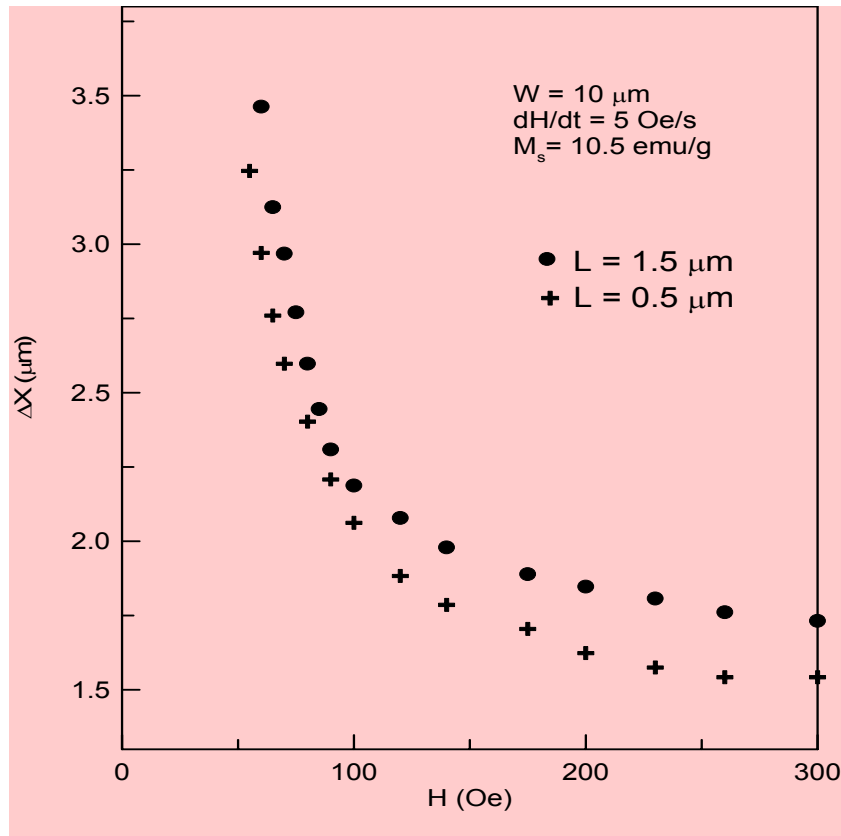


Fig.12.  $\Delta x$ - $H$  curve moves toward the lower left, when  $W$  is decreased

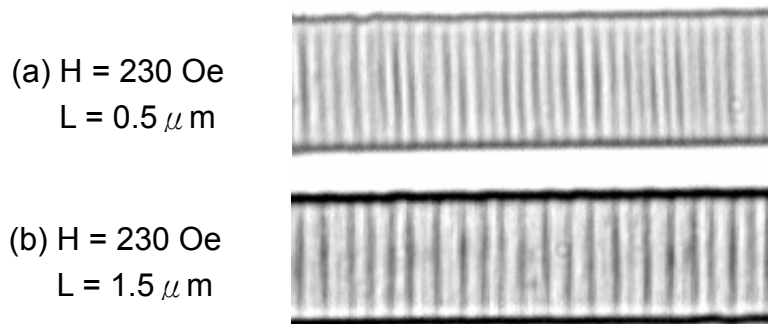


Fig.13. Periodic chain under a given  $H$  for various  $L$

In summary, a one dimensional ordered structure can be achieved in magnetic fluid films under parallel magnetic fields. This ordered structure is tunable and can be well manipulated by controlling field strength, sweep rate, fluid concentration, cell width and film thickness. The relevant control method have been demonstrated in the following, we would like to further discuss the physical intuition of the tunability of the ordered structure in the magnetic fluid film under parallel fields.

## **VI. Discussion on the tunability of ordered structure in a magnetic fluid film.**

When a parallel magnetic field was applied to the magnetic fluid micro-strip, versatile structural patterns were observed. Under lower field strength, no patterns can be found in the magnetic fluid film until the field strengths exceeds a critical value, the magnetic particles which were originally dispersed in the fluid ,start to agglomerate to form magnetic chains, as shown by the black bars in Fig. 4(a). It is worth that all of chains in the micro-strip are nearly identical and possess have almost the same length, which corresponds to the width of the cell. This phenomenon is much clearer for higher fields, as shown in Fig. 4(d). Under lower fields, these magnetic chains are distributed randomly in the micro-strip because there are few chains and the interactions between them are too weak. With the increase of the field strength, more and more columns appear and they become closer together. Since these identical chains are magnetic and their magnetic moments are parallel (along the field direction), the reduction in the spacing between the chains leads to an enhancement of the interaction between the chains. In order to achieve a minimum energy in the system of magnetic chains, A one-dimensional ordered structure results under a higher field, as shown in Fig. 4(a). As the field strength is further raised, the chain spacing is reduced because of the formation of new chains, as shown in Figs. 4(b)-4(d). A

quantitative analysis of the field-dependent chain spacing,  $\Delta x$ -H curve, is shown in Fig.5.

In Fig. 5, a rapid decrease in  $\Delta x$  from 3.40 to 2.16  $\mu\text{m}$  as H is raised from 60 to 100 Oe, and then the  $\Delta x$  was further reduced gradually, increasing H over 100 Oe. The results shown in Fig. 5 clearly reveal that the one-dimensional ordered structure in the magnetic fluid micro-strip is tunable by adjusting the external field strength. In addition, the observed minimum value of the chain spacing  $\Delta x$  ( $= 1.73 \mu\text{m}$ ) under the highest field ( $= 300 \text{ Oe}$ ) in this work is larger than the depth of the cell ( $= 1.5 \mu\text{m}$ ). Thus, the architecture of a single -layer is obtained for the one-dimensional tunable ordered structure of magnetic chains in the magnetic fluid micro-strip under parallel fields.

To realize the physical intuition in the tunability of the one-dimensional ordered structure in the magnetic fluid strip, we propose a model and then calculate the relationship between the  $\Delta x$  and H. As indicated above, the ordered structure in the magnetic fluid micro-strip can be regarded as a one-dimensional array of identical magnetic chains under external magnetic fields. Thus, this array can be represented by the scheme shown in Fig. 14(a). Each magnetic chain is treated as a magnetic cylinder with a magnetic moment  $M$ , which is parallel to the external field  $H$ , and each is assumed to be uniform inside a magnetic cylinder. The height of the cylinder corresponds to the width of cell  $W$ , and the cylinder spacing is denoted by  $\rho$ . It is also noted that, under a given  $H$ , the  $\rho$  reverts to the observed  $\Delta x$  as the system reaches minimum energy level.

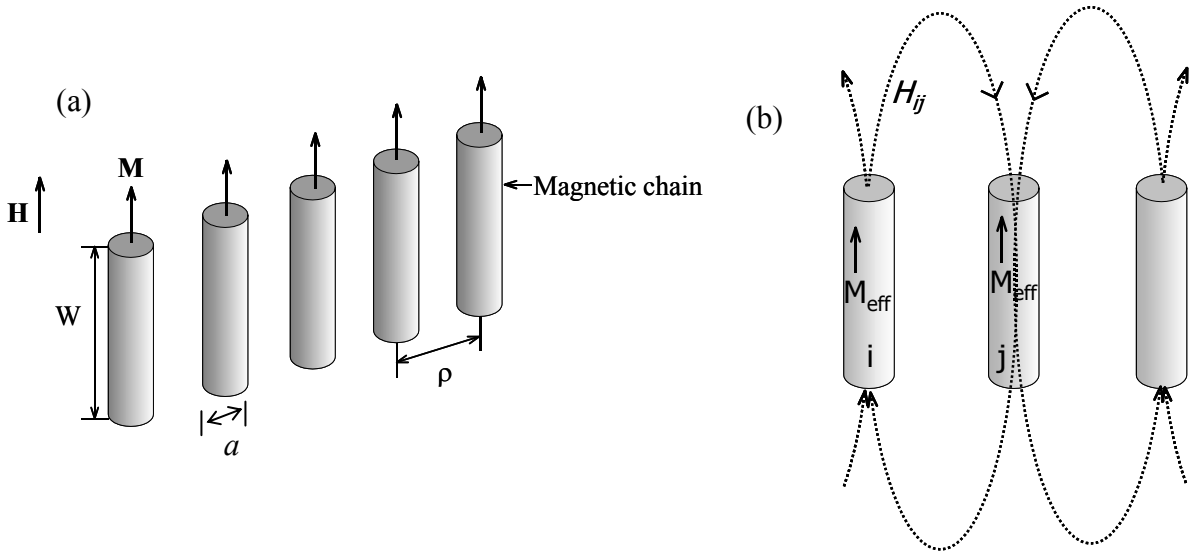


Fig.14. Scheme for (a) modeling of the one-dimensional ordered structure of magnetic chains in the magnetic fluid micro-strip and (b) interaction between two neighboring magnetic chains

In principle, there are three main physical interactions in this system: one is thermal energy, another is the attractive interaction between the magnetic chains and the external magnetic field, the third is that among magnetic chains. According to our previous study,<sup>19</sup> the thermal energy of the magnetic nano-particle in the liquid at room temperature is depressed by its magnetic potential energy under an applied field strength. Thus, the contribution of thermal energy to the total energy of the system is negligible. The other energies due to magnetic interactions are then considered into account for the tunability of the ordered structure in the magnetic micro-strip.

The attractive interaction between the magnetic chains and the external field leads to the negative magnetic potential energy,  $U_{\text{cH}}$ . In the theoretical calculations, we assume the strip cell is infinitely long because of the cell length (several mm's) is much larger than the chain spacing (several  $\mu\text{m}$ 's). Hence, the  $U_{\text{cH}}$  can be represented in terms of the magnetic potential energy density per unit length along the strip cell and can be expressed as

$$U_{\text{cH}} = nu_{\text{cH}}, \quad (1)$$

where  $n$  denotes the numbers of chains per unit length along the strip cell, and is equal to  $1/\rho$ , and  $u_{cH}$  is the magnetic potential of a single magnetic chain under an external field, and is  $-M_{\text{eff}}H$ , where the  $M_{\text{eff}}$  is the effective magnetic moment of each magnetic chain considering the demagnetization effect. Therefore, Eq. (1) becomes

$$U_{cH} = -M_{\text{eff}}H/\rho \quad (2)$$

For the repulsive interaction between two magnetic chains with parallel magnetic moments, the resultant magnetic potential energy density is positive and can be evaluated via

$$U_{cc} = \frac{n}{2} \sum_{s \text{ integer}} 2u_{cc}(s\rho), \quad (3)$$

where  $u_{cc}(s\rho)$  is the magnetic potential energy of two magnetic chains, separated by a distance of  $s\rho$  with  $s$  being the positive integer because of the periodicity of the ordered structure. For each chain, there is always two chains separated from it by a distance of  $s\rho$ . This fact leads to the factor 2 in the summation of Eq. (3). For simplicity, the contribution to  $u_{cc}$  of a certain chain from the first nearest neighboring chain is considered. The value of  $u_{cc}(\rho)$  can be obtained via

$$u_{cc}(\rho) = -\int_j \mathbf{H}_{ij}(\rho) \cdot d\mathbf{M}_{j\text{eff}}, \quad (4)$$

where  $H_{ij}$  denotes the magnetic field, which is generated by chain  $i$ , at chain  $j$  shown in Fig. 14(b), and  $dM_{j\text{eff}}$  is a segment of the effective magnetic moment inside chain  $j$ . Significantly, the directions of  $H_{ij}$  and  $dM_{j\text{eff}}$  are anti-parallel, so  $u_{cc}$  is positive. With Eqs. (2) – (4), the total energy density along the strip cell can be written as

$$\begin{aligned} U_T &= U_{cH} + U_{cc} \\ &= -M_{\text{eff}}H/\rho + \left(-\int_j \mathbf{H}_{ij}(\rho) \cdot d\mathbf{M}_{j\text{eff}}\right)/\rho \end{aligned} \quad (5)$$

It is clear that  $U_T$  is a function of  $\rho$ . Moreover, under a given  $H$ , the

value of the first term in Eq. (5) decreases for a smaller  $\rho$ , whereas the second term becomes larger. Thus, the contributions to the total energy density from these two compensate for each other, which implies that there exists an equilibrium state for the system. The chain spacing at the equilibrium state under a given  $H$  can be obtained by equating the differential of the total energy density with respect to  $\rho$  to be zero, i.e.  $dU_T/d\rho|_{\rho=\Delta x} = 0$ . From doing the differential and through a calculation process, we obtain

$$H=M_{\text{eff}} f(a,W,\Delta x), \quad (6)$$

where  $a$  is the diameter of a cylinder shown in Fig. 14(a). Equation (6) is a theoretical relationship between the  $\Delta x$  and  $H$ . We then use the experimental data from  $a, W, \Delta x$ , and  $H$  shown in Fig. 5 to plot the  $H$ - $f$  curve, as denoted by the data points in Fig.15. These data are fitted to Eq. (6) with the fitting parameter  $M_{\text{eff}}$ . It was found that the data points merge with the theoretical curve when  $H$  is higher than 140 Oe, whereas there is a deviation of the data points from the theoretical relationship for  $H$  exist from 60 to 140 Oe. This deviation may be because that the ordering of the structure in the magnetic fluid film under  $H$ , from 60 to 140 Oe, is not high enough, as indicated by the structural picture shown in Fig. 4(b) and 4(c). Hence, this kind of structural pattern can be referred to as a quasi-ordered structure. A perfect ordered structure is achieved under  $H$  higher than 140 Oe, as shown in Fig. 4(d).

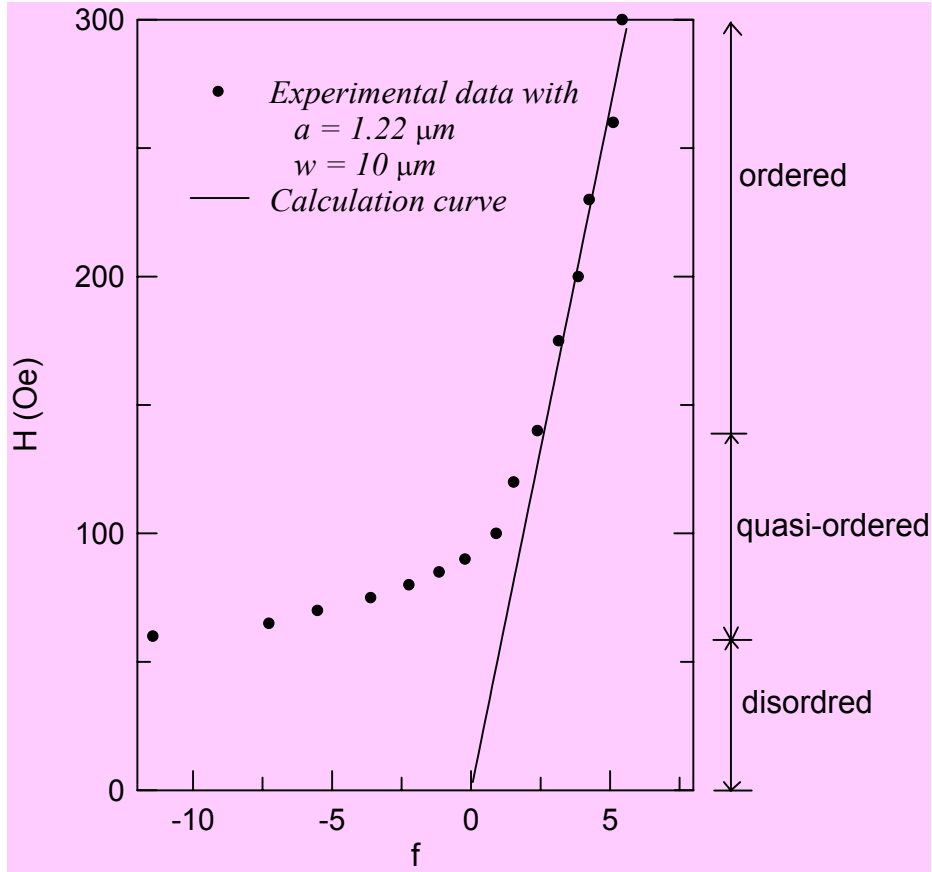


Fig.15. Comparison between the experimental data and the calculated curve from Eq. (6) for the one-dimensional structural patterns in the magnetic fluid micro-strip under parallel magnetic fields.

## VII. Conclusions

- A. The tunable one-dimensional ordered structure is demonstrated in the magnetic fluid films under parallel magnetic fields.
- B. This ordered structure can be well manipulated ,The results show that the structure period  $\Delta x$  can be reduced by controlling factors such as enhancing  $H$  (external magnetic field),  $dH/dt$  (magnetic field sweeping rate),  $M_s$  (concentration of magnetic fluid) or by reducing  $W$  (cell width ) and  $L$  (film thickness).
- C. By conducting a comparison on the theoretical computation and the experimental results, we ensure that in this system, there are

two major physical interactions: (1) The magnetic energy  $U_{ch}$  between magnetic chains and the external magnetic field; (2) The magnetic energy  $U_{cc}$  aroused from the repulsion between two magnetic chains magnetized in the same direction.

## VIII. Acknowledgement

I sincerely thank Prof. Heng-Er Horng in National Taiwan Normal University for her super advise.

## Reference

1. R.E Rosensweig, Nature, **210**, 613(1966).
2. G.A. Jones and H. Niedoba, J. Magn. Mater., **73**, 33(1988).
3. Hao Wang, Yun Zhu, C. Boyd, Weili Luo, A. Cebers, and R.E. Rosensweig, Phys. Rev. Lett., **72**, 1929(1994).
4. Susamu Taketomi, Hiromasa Takahashi, Nobuyuki Inaba, and Hideki Miyajima, J. Phys. Soc. Jap., **60**, 1689(1991).
5. Chin-Yih Hong, H.E. Horng, I.J. Jang, C.J. Hsu, Y.D. Yao, and H.C. Yang, J. Appl. Phys., **81**, 4275(1997).
6. Chin-Yih Hong, Heng-Er Horng, F.C. Kuo, S.Y. Yang, H.C. Yang, and J.M. Wu, Appl. Phys. Lett., **75**, 2196(1999).
7. S.Y. Yang, H.Z. Horng, Chin-Yih Hong, H.C. Yang, M.C. Chou, C.T. Pan and Y.H. Chao, J. Appl. Phys., **93**, 3457(2003).
8. Chin-Yih Hong, C.H. Ho, H.E. Horng, Chun-Hui Chen, S.Y. Yang, Y.P. Chiu, and H.C. Yang, Magnetohydrodynamics, **35**, 297(1999).
9. S.Y. Yang, Y.H. Ke, W.S. Tse, H.E. Horng, Chin-Yih Hong, and H.C. Yang, J. Magn. Mater., **252**, 290(2002).
10. Heng-Er Horng, Chin-Yih Hong, Wai Bong Yeung, and Hong-Chang Yang, Appl. Opt., **37**, 2674(1998).

11. Heng-Er Horng, S.Y. Yang, S.L. Lee, Chin-Yih Hong, and H.C. Yang, *Appl. Phys. Letter.*, **79**, 350(2001).
12. S.Y. Yang, Y.P. Chiu, H.E. Horng, Chin-Yih Hong, B.Y. Jeang, and H.C. Yang, *Appl. Phys. Lett.*, **79**, 2372(2001).
13. S.Y. Yang, Y.F. Chen, H.E. Horng, Chin-Yih Hong, W.S. Tse, and H.C. Yang, *Appl. Phys. Lett.*, **81**, 4931(2002).
14. H.E. Horng, Chin-Yih Hong, S.L. Lee, C.H. Ho, S.Y. Yang, and H.C. Yang, *J. Appl. Phys.*, **88**, 5904(2000).
15. Jong-Wook Seo, Sang Ju Park, and Kyeong Oh Jang, *J. Appl. Phys.*, **85**, 5956(1999).
17. Chin-Yih Hong, *J. Appl. Phys.*, **85**, 5962(1999).
18. Nihad A. Yusuf, *J. Phys. D: Appl. Phys.*, **22**, 1961(1989).
19. S. Taketomi, S. Ogawa, H. Miyajima, and S. Chikazumi, *IEEE Trans. Magn.*, **4**, 384(1989).
20. H.E. Horng, Chin-Yih Hong, H.C. Yang, I.J. Jang, S.Y. Yang, J.M. Wu, S.L. Lee, and F.C. Kuo, *J. Magn. Magn. Mater.*, **201**, 215(1999).
21. S.Y. Yang, I.J. Jang, H.E. Horng, Chin-Yih Hong, and H.C. Yang, *Magnetohydrodynamics*, **36**, 16(2000).

## 評語

作者從事科學實驗的態度相當積極而仔細。以高一學生的程度及時間而言，能對許多新接觸的儀器操作及原理有相當程度的認識及運用，在努力及能力方面都值得嘉許。